Scientific Research and Essays

Volume 9 Number 19 15 October 2014
ISSN 1992-2248

Academic Journals

ABOUT SRE

The **Scientific Research and Essays (SRE)** is published twice monthly (one volume per year) by Academic Journals.

Scientific Research and Essays (SRE) is an open access journal with the objective of publishing quality research articles in science, medicine, agriculture and engineering such as Nanotechnology, Climate Change and Global Warming, Air Pollution Management and Electronics etc. All papers published by SRE are blind peer reviewed.

Submission of Manuscript

Submit manuscripts as e-mail attachment to the Editorial Office at: sre@academicjournals.org. A manuscript number will be mailed to the corresponding author shortly after submission.

The Scientific Research and Essays will only accept manuscripts submitted as e-mail attachments.

Please read the **Instructions for Authors** before submitting your manuscript. The manuscript files should be given the last name of the first author.

Editors

Editorial Board

n detail.

Fees and Charges: Authors are required to pay a $550 handling fee. Publication of an article in the Scientific Research and Essays is not contingent upon the author's ability to pay the charges. Neither is acceptance to pay the handling fee a guarantee that the paper will be accepted for publication. Authors may still request (in advance) that the editorial office waive some of the handling fee under special circumstances.

Submission of a manuscript implies: that the work described has not been published before (except in the form of an abstract or as part of a published lecture, or thesis) that it is not under consideration for publication elsewhere; that if and when the manuscript is accepted for publication, the authors agree to automatic transfer of the copyright to the publisher.

Scientific Research and Essays

Table of Contents: Volume 9 Number 19 15 October, 2014

ARTICLES

Research Articles

academicJournals

Vol. 9(19), pp. 834-839, 15 October, 2014
DOI: 10.5897/SRE2014.6081
Article Number: 8C4E06A48079
ISSN 1992-2248 © 2014

http://www.academicjournals.org/SRE

Scientific Research and Essays

Full Length Research Paper

Influence of post-fire successional gradients in *Pinus brutia* forests on ground beetle community changes

Burçin Yenisey Kaynaş

Department of Biology, Faculty of Arts and Science, Mehmet Akif Ersoy University, İstiklal Campus, Burdur/Turkey.

Received 15 August, 2014; Accepted 26 September, 2014

Fire is a common disturbance factor in Mediterranean ecosystems. It is a very spectacular ecological force because it destroys ecosystems in a very short time. Insect groups are commonly used as indicators to evaluate habitat changes after disturbances. In this study, the successional changes were evaluated by the composition of ground beetles communities in East Mediterranean pine forests. Ground beetle fauna was investigated using pit-fall traps at 17 sampling sites in *Pinus brutia* forests burned in different times. Plant species richness, vegetation and surface characteristics were measured as microhabitat variables in the study sites and the relationships between ground beetle abundance and microhabitat variables were estimated with Pearson Correlation Analysis. As a result, it was determined that recolonization of ground beetle communities did not occur in early successional stages. In the sites burned 9, 16 and 26 years ago, that represent middle and late successional stages, the abundance and species richness of Carabidae were higher and then decrease again in mature pine forest. The relationships between microhabitat parameters and Carabidae abundance were estimated and changes of ground beetle communities depending on microhabitat structure were not determined.

Key words: Carabidae, disturbance, Mediterranean, succession, fire.

INTRODUCTION

Fire is a common feature of Mediterranean landscapes (Bilgili and Sağlam, 2003). Vegetation composition and structure in Mediterranean type ecosystems are strongly shaped by the fire regime (Díaz-Delgado et al., 2002; Radea and Arianoutsou, 2000; Trabaud, 2000). Post fire regeneration of vegetation in every level of biological organisation hierarchies and life-hisory traits has been studied intensively (Thanos et al., 1989; Ne'eman et al., 1992; Spanos et al., 2000).

Changes of forest habitat structure and vegetation after disturbance make lead changes in the structure and dynamics of faunal communities. The effects of fire on faunal communities and changes of faunal community dynamics after fire concentrated on more affects especially to insects and small mammals (Prodonet al., 1987; Haim and Izhaki, 2000; Kaynaş and Gurkan, 2008). Effects of fire on insects and other arthropods can operate through a variety of mechanisms at different temporal scales (Andersen and Müller, 2000). Direct effects of fires include mortality, forced emigration (Whelan, 1995), or immigration of pyrophilous insects that are favored by fire (Wikars, 2002; Wikars and Schimmel, 2001). Indirect effects of fire mostly depend on vegetational changes. Following fire, changes of plant

E-mail: bykaynas@mehmetakif.edu.tr, Tel: +902482133052.

Table 1. Locations and altitutes of sampling sites.

Successional age	Replication sites	Locations	Altitudes (m)
3	1	36° 59' 24" N, 28° 20' 05" E	217
	2	36° 59' 30" N, 28° 20' 05" E	175
	3	36° 59' 33" N, 28° 19' 23" E	105
6	1	36° 50' 17" N, 28° 18' 02" E	55
	2	36° 50' 08" N, 28° 18' 08" E	35
	3	36° 49' 53" N, 28° 18' 30" E	35
9	1	36° 55' 43" N, 28° 12' 14" E	105
	2	36° 55' 42" N, 28° 12' 12" E	80
	3	36° 53' 44" N, 28° 11' 49" E	35
16	1	36° 58' 50" N, 28° 18' 53" E	185
	2	36° 58' 57" N, 28° 18' 46" E	140
	3	36° 59' 05" N, 28° 18' 25" E	125
26	1	36° 49' 58" N, 28° 20' 25" E	180
	2	36° 49' 51" N, 28° 20' 00" E	150
	3	36° 49' 20" N, 28° 19' 05" E	90
50<	1	36° 50' 54" N, 28° 17' 42" E	55
	2	36° 54' 24" N, 28° 10' 36" E	35

species composition, plant diversity (Lawton, 1983; Siemann, 1998; Siemann et al., 1999) and plant architecture (Southwood et al., 1979; Lawton, 1983) influence the diversity and richness of insect communities. In Mediterranean ecosystems, the changes of plant architecture and vegetation structure should be more important on insect community change (Kaynaş and Gürkan, 2008), because re-establishment of the pre-fire plant communities is rapid (Trabaud, 1994) and there is no real succession in the sense of replacement of species or communities (Keeley, 1986; Trabaud, 2000).

Carabid beetles are among the best studied taxa regarding microhabitat changes. They are used as indicator group for the evaluation of the effects of habitat fragmentation (Magura et al., 2004), different types of disturbance (Latty et al., 2006; Ribera et al., 2001), forestry applications (Heliola et al., 2001), and classification of landscapes (Rykken et al., 1997). They are appropriate subjects for such studies because they are diverse and abundant, taxonomically well-known and sensitive to habitat changes (Niemalä et al., 1993, 1992, 1988).

In this research we aimed to study the changes of Carabid communities during post-fire successions and microhabitat features which influence the Carabid communities in this period.

MATERIALS AND METHODS

The study was conducted in several *Pinus brutia* Ten. 1815 forests with many areas affected by fire in different degree (as a result of being burned in different years). These forests are located at Marmaris district (36°50' N, 28°17' E) and its surrounding areas, which is situated on the Mediterranean coast of southwestern Turkey. This area has a typical Mediterranean climate with a hot and dry summer. The total precipitation is 1211.7 mm year^{-1} (between 1975 and 2006), with a dry period that lasts for 5 months, between May and September. Monthly mean temperatures range from 10.6°C in January to 28.3°C in July. The vegetation on the area is mostly represented by *Pinus brutia* forests; other major vegetation types are Maquis, Phrygana and *Liquidambar orientalis* Mill.1768 forests.

For the samplings, the areas were selected in order to cover the major range of successional gradient of forest recuperation after the effects of a fire, by choosing areas burned with natural fires 3, 6, 9, 16 and 26 years ago and areas that has not been affected by fire for a longer period (>50 years). The samplings were made in three replication sites for every successional stage and two for unburned areas. The dominant vegetation types of all sites was *P. brutia* forest and all the samplings stretches from an altitude of 0 to 250 m (Table 1).

Ground beetles were sampled during a three-days period in March, May, June and August of 2005, using pit-fall traps. The traps consisted of plastic jars with a diameter of about 7 cm buried in the soil up to the brink and half filled with 30% ethylene alcohol. Sixteen pitfall traps were placed at each site in a 4x4 grid with 10 m intervals between each trap.

Microhabitat structure of the sites was analyzed with the point quadrats technique (Sutherland, 2006). For each trap locations, nine points were selected, one of these was center and remaining eight were situated in four different directions around the trap (Figure 1). In every point, the plant species were identified, the height of plant at this point was measured and surface characteristics were recorded.

After emptying, each individual was mounting and equipped with cardboard label identifying its trap number, site name and sampling

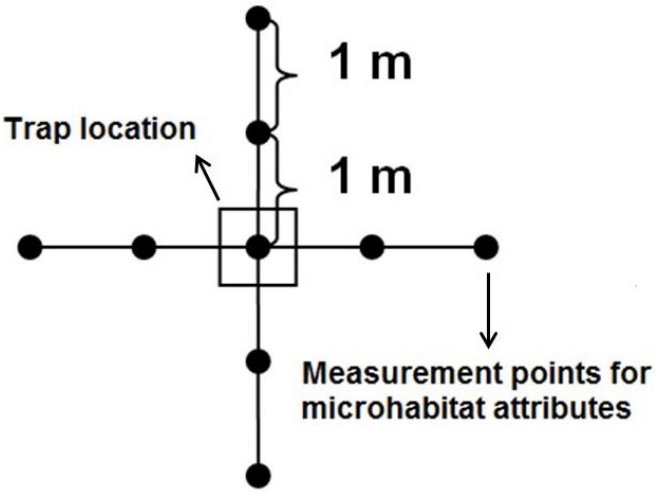

Figure 1. Sampling design for microhabitat attributes in each trap locations

time before preserving in wooden drawers. They were identified to species level in Entomology Laboratory at Hacettepe University.

Species richness and abundance of successional sites were estimated by calculating arithmetic average of number of species and individuals of replication sites respectively.

The habitat structure of the study sites was evaluated from vegetation and surface characteristics. The parameters about vegetation were: Plant species richness, mean height of vegetation, stratification and cover of vegetation, and were calculated for every replication sites.

The overlap ration of plants at one sampling point can be used expression of vertical stratification in a habitat. In a point of forest habitat, a subshrub, a shrub and a tree can be found together in the same point vertically and stratification increase with increasing number of plants in a sampling point. Vegetation stratification was calculated by total number of counted plants to sampling points (9) for each trap location. Vegetation cover is expression of cover area of plants on surface and it was estimated by dividing numbers of points which were occupied any plants (not empty points) to total sampling points.

Surface characteristics were analyzed at the same trap locations. Surface structure was evaluated in terms of soil, stone, rock, leaf, branch and needle. Surface complexity was estimated by calculating the mean of component numbers at a measure point.

The number of variables to be analyzed was reduced by applying a principal component analysis (PCA) on all the variables that resulted highly correlated. After all of these variables were reduced with Principal Component Analysis, calculating scores and abundance of Carabidae of all sites was done with Pearson Correlation Analysis (SPSS Statistics 17.0).

RESULTS

A total of 29 individuals belonging to 10 species of ground beetles were captured in 4080 trap/nights. With respect to changes of Carabid communities depending on successional gradient, we see that abundance and species richness of ground beetle communities was very low in early successional stages and they progressively increase towards middle and late successional stages. In unburned forest these values decrease again. The sites burned 3 and 6 years ago were represented by a very small number of species and individuals. The sites burned 9, 16 and 26 years ago have relatively higher species richness and abundance compared the other sites (Figure 2). The species with the highest rate of capture was *Leistus rufomarginatus* (Duftschmid, 1812). *Carabus graecus morio* (Mannerheim, 1830) and *Ditomus calydonius* (Rossi, 1790) were also common. While *C. graecus morio* did not display any change depending on successional gradient, *D. calydonius* was captured only in middle and late successional stages. The other species were captured in very small numbers and generally appears in only one of the sampled successional stages (Table 2).

Principal component analysis displayed that the cumulative percentage of variance for the three axes was 80.3%. The first axes was highly correlated with characters peculiar to late successional stages such as total plant species richness, habitat stratification, cover and height of vegetation and needle cover. Second axes were relevant with two variables cover leaf and branch, third one was rock cover. Because correlation coefficients between total Carabid abundance and obtained three axes were very low (Pearson correlation coefficients; 1. Axes: 0,121; 2. Axes: -0,110; 3. Axes: 0,018), no significant relationship was found between microhabitat variables and Carabid abundance.

DISCUSSION

In Mediterranean region, plant communities which have been shaped with fire for thousands of years are resilient, with different regeneration strategies (Keeley, 1986). Although ground beetles were stated as resilient for prairie habitats (Cook and Holt, 2006), an early regeneration of ground beetle communities seems not to be the case in this study for *P. brutia* forests. In early stages of succession, ground beetle communities were represented by very few individuals and species. This result may be due to species still have to colonize in significant numbers. The retardation in colonization may occur for ground beetles communities at recently opened areas (Niemelä et al., 1993; Saint-Germain et al., 2005). In stressed climatic conditions like Mediterranean ecosystems, open habitats can limit colonization and activation of ground beetles. Greater temperature fluctuations and reduced humidity levels may disturb the invertebrate community (Pearce and Venier, 2006). Vegetation cover may have an important role in protecting Carabidae from direct insulation and desiccation and a decrease in vegetation and litter cover have a negative impact on surface moisture (Barone and Frank, 2003). A suitable humidity condition, provided by vegetation cover, is important for ground beetles in habitat preference (Thiele, 1977). The reduction in the

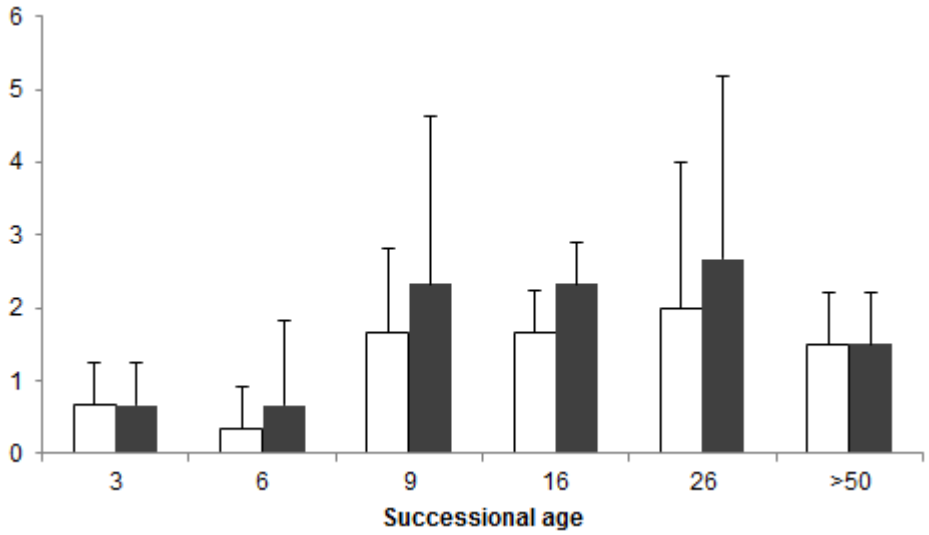

Figure 2. Mean species richness (open bar) and abundance (solid bar) of ground beetless in successional stages after fire.

Table 2. Total number of individuals of Carabid beetles at successional stages after fire.

Species	Years after fire					
	3	**6**	**9**	**16**	**26**	**>50**
Bembidion tetracolum			1			
Calathus melanocephalus						1
Calosoma reticulatum				2		
Carabus graecus morio		2	3		1	1
Cymindis lineata			1			
Ditomus calydonius				2	2	
Leistus ferrugineus					1	
Leistus rufomarginatus	2			2	4	1
Ocydromus sp.			1			
Pterostichus sp.			1	1		

amount of tree leaf litter may have contributed to the reduced abundance of taxa that requires shelter, moisture, and food provided by tree leaf litter (Blanche et al., 2001).

Mediterranean ecosystems is known resilient to fire and re-establishment of the pre-fire communities is very rapid (Trabaud, 1994). Even if there is no change in species composition of plant community with time after fire, vegetation characteristics such as height, cover display to change with successional gradient in post-fire areas (Tavşanoğlu and Gürkan, 2014). In this study, no relationship was determined between habitat variables and Carabid abundance. Similarly Chapman (2014) stated that level of heterogeneity in habitat structure did not have a great influence in Carabid communities. To make a certain interpretation like this is impossible because remarkable low number of individuals belong to Carabid communities for this study. Although a clear association was not detected in here, the importance of habitat structure in Carabid community structure was revealed in many studies.

The increase in habitat heterogeneity with successional age depends on vegetation height (Kruess and Tscharntke, 2002) and heterogeneity of vegetation was a better predictor of Carabidae species richness than plant species diversity (Brose, 2003). The importance of habitat heterogeneity was displayed in some studies (Sroka and Finch, 2006). Complex habitats, respect of floristic and physical features, create a preferable microclimate for ground beetles (Larsen et al., 2003; Lassau et al., 2005). In addition Shelef and Groner (2011) stated that beetle behavior is affected by shrub structure and beetles use shrub shading for their thermoregulation. In this respect the middle aged sites in

successional gradient had a higher shrub cover and could be more suitable habitats for ground beetles. However, mature forest unburned for very long time had complex habitat attributes and display low abundance and species richness value in comparison to middle and late successional stages. In studies carried out in the same ecosystems, Kaynaş and Gürkan (2007) stated the negative impact of closed canopy structure of vegetation on some insect groups. Middle and late successional stages had heterogenous environments depend on increase vegetation height and lack of closed canopy closure constitutes favorable habitats for ground beetles.

In conclusion, despite such a tendency with successional gradient in communites of Carabidae, low number of species and the lack of correlation between Carabid correlation and habitat variables obstructed to make certain evaluations. In Mediterranean ecosystems, there is limited knowledge about subjects of interactions between fire and insects, and adaptations of insect communities to fire-induced habitat alterations. Long-term studies are needed for comprehensive and accurate evaluations.

Conflict of Interest

The authors have not declared any conflict of interest.

ACKNOWLEDGEMENTS

The author thank Neslihan Kocatepe for identification specimens. She also thank Sinan Kaynaş, Çağatay Tavşanoğlu, Anıl Soyumert, Oksal Macar, Filiz Yeni, Yasin İlemin, Okan Ürker, and Hüseyin Yılmaz for helps in the field. Funding and support for this research were provided by the Hacettepe University, Scientific Research Unit (Project no: 02.02.601.004).

REFERENCES

Andersen AN, Muller WJ (2000). Arthropod responses to experimental fire regimes in an Australian tropical savannah; ordinal-level analysis. Austral Ecol. 25(2):199-209. http://dx.doi.org/10.1046/j.1442-9993.2000.01038.x

Barone M, Frank T (2003). Habitat age increases reproduction and nutritional condition in a generalist arthropod predator. Oecologia 135(1):78-83. http://dx.doi.org/10.1007/s00442-002-1175-2

Bilgili E, Saglam B (2003). Fire behavior in maquis fuels in Turkey. Forest Ecol. Manag.184:201-207. http://dx.doi.org/10.1016/S0378-1127(03)00208-1

Blanche KR, Andersen AN, Ludwig JA (2001). Rainfall-contingent detection of fire impacts: responses of beetles to experimental fire regimes. Ecol. Appl. 11(1):86-96. http://dx.doi.org/10.1890/1051-0761(2001)011[0086:RCDOFI]2.0.CO;2

Brose U (2003). Bottom-up control of Carabid beetle communities in early successional wetlands: mediated by vegetation structure or plant diversity? Oecologia 135:407-413. http://dx.doi.org/10.1007/s00442-003-1222-7

Chapman A (2014). The influence of landscape heterogeneity - ground beetles (Coleoptera:Carabidae) in Fthiotida, central Greece. Biodiversity Data Journal 2: e1082. http://dx.doi.org/10.3897/BDJ.2.e1082

Cook WM, Holt RD (2006). Fire frequency and mosaic burning effects on a tall grass prairie ground beetle assemblage. Biodivers. Conserv. 15:2301-2323. http://dx.doi.org/10.1007/s10531-004-8227-3

Díaz-Delgado R, Lloret F, Pons X, Terradas J (2002). Satellite evidence of decreasing resilience in Mediterranean plant communities after recurrent wild fires. Ecol. 83:2293-2303. http://dx.doi.org/10.1890/0012-9658(2002)083[2293:SEODRI]2.0.CO;2

Haim A, Izhaki I (2000). The effect of different treatments on the community composition of small mammals in a post-fire pine forest. J. Mediterr. Ecol. 1:249-257.

Heliola J, Koivula M, Niemelä J (2001). Distribution of Carabid beetles (Coleoptera, Carabidae) across a Boreal forest-clearcut ecotone. Conserv. Biol. 15(2):370-377. http://dx.doi.org/10.1046/j.1523-1739.2001.015002370.x

Kaynaş BY, Gurkan B (2007). Species diversity of butterflies in *Pinus brutia* forest ecosystems after fire. Entomol. News 118(1):31-40. http://dx.doi.org/10.3157/0013-872X(2007)118[31:SDOBIT]2.0.CO;2

Kaynaş BY, Gurkan B (2008). Species richness and abundance of insects during post-fire succession of a *Pinus brutia* forest in Mediterranean region. Pol. J. Ecol. 56(1):165-172. http://www.pje.miiz.waw.pl/

Keeley JE (1986). Resilience of mediterranean shrub communities to fires. In Resilience in Mediterranean-type ecosystems, edited by Dell B, Hopkins AJM, Lamont BB, Dr W. Junk Publishers, Dordrecht, pp. 95-112. http://dx.doi.org/10.1007/978-94-009-4822-8_7

Kruess A, Tscharntke T (2002). Grazing intensity and the diversity of grasshoppers, butterflies, and trap-nesting bees and wasps. Conserv. Biol. 16:1570-1580. http://dx.doi.org/10.1046/j.1523-1739.2002.01334.x

Larsen KJ, Work TT, Purrington FF (2003). Habitat use patterns by ground beetles (Coleoptera: Carabidae) of northeastern Iowa. Pedobiologia 47:288-299. http://dx.doi.org/10.1078/0031-4056-00192

Lassau SA, Hochuli DF, Cassis G, Reid CAM (2005). Effects of habitat complexity on forest beetle diversity: do functional groups respond consistently? Divers. Distrib. 11:73-82. http://dx.doi.org/10.1111/j.1366-9516.2005.00124.x

Latty EF, Werner SM, Mladenoff DJ, Raffa KF, Sickley TA (2006). Response of ground beetle (Carabidae) assemblages to logging history in northern hardwood-hemlock forests. Forest Ecol. Manag. 222:335-347. http://dx.doi.org/10.1016/j.foreco.2005.10.028

Lawton JH (1983). Plant architecture and the diversity of phytophagous insects. Annu. Rev. Entomol. 28:23-39. http://dx.doi.org/10.1146/annurev.en.28.010183.000323

Magura T, Tóthmérész B, Molnár T (2004). Changes in carabid beetle assemblages along an urbanisation gradient in the city of Debrecen, Hungary. Landscape Ecol. 19:747-759. http://dx.doi.org/10.1007/s10980-005-1128-4

Ne'eman G, Lahav H, Izhaki I (1992). Spatial pattern of seedlings 1 year after fire in a Mediterranean pine forest. Oecologia 91:365-370. http://dx.doi.org/10.1007/BF00317625

Niemalä J, Langor D, Spence JR (1993). Effects of clear-cut harvesting on Boreal ground-beetle assemblages (Coleoptera: Carabidae) in western Canada. Conserv. Biol. 7(3):551-561. http://dx.doi.org/10.1046/j.1523-1739.1993.07030551.x

Niemalä J, Haila Y, Halme E, Pajunen T, Punttila P (1992). Small-scale heterogeneity in the spatial distribution of Carabid beetles in the southern Finnish taiga. J. Biogeogr. 19:173-181. http://dx.doi.org/10.2307/2845503

Niemalä J, Haila Y, Halme E, Lahti T, Pajunen T, Punttila P (1988). The distribution of Carabid beetles in fragments of old coniferous taiga and adjacent managed forests. Ann. Zool. Fenn. 25:107-119. http://www.sekj.org/PDF/anzf25/anz25-107-119.pdf

Pearce JL, Venier LA (2006). The use of ground beetles (Coleoptera: Carabidae) and spiders (Araneae) as bioindicators of sustainable forest management: A review. Ecol. Indic. 6:780-793. http://dx.doi.org/10.1016/j.ecolind.2005.03.005

Prodon R, Fons R, Athias-Binche F (1987). The impact of fire on animal communities in Mediterranean Area. In The Role of Fire in Ecological

Systems edited by Trabaud L, SPA Academic Publishing, The Hague, pp. 121-157.
Radea C, Arianoutsou M (2000). Cellulose decomposition rates and soil arthropod community in a *Pinus halepensis* Mill. forest of Greece after wildfire. Eur. J. Soil Biol. 36(1):57-64. http://dx.doi.org/10.1016/S1164-5563(00)01045-1
Ribera I, Doledec S, Downie IS, Foster GN (2001). Effect of land disturbance and stress on species traits of ground beetle assemblages. Ecology 82:1112-1129. http://dx.doi.org/10.1890/0012-9658(2001)082[1112:EOLDAS]2.0.CO;2
Rykken J, Capen DE, Mahabır SP (1997). Ground beetles as indicators of land type diversity in the Green Mountains of Vermont. Conserv.Biol. 11:522-530. http://dx.doi.org/10.1046/j.1523-1739.1997.95336.x
Saint-Germain M, Larrivée M, Drapeau P, Fahrig L, Buddle CM (2005). Short-term response of ground beetles (Coleoptera: Carabidae) to fire and logging in a spruce-dominated boreal landscape. Forest Ecol. Manag. 212:118-126. http://dx.doi.org/10.1016/j.foreco.2005.03.001
Shelef O, Groner E (2011). Linking landscape and species: Effect of shrubs on patch preference of beetles in arid and semi-arid ecosystems. J. Arid Environ. 75:960-967. http://dx.doi.org/10.1016/j.jaridenv.2011.04.016
Siemann E, Haarstad J, Tilman D (1999). Dynamics of plant and arthropod diversity during old field succession. Ecography 22(4):406-414. http://dx.doi.org/10.1111/j.1600-0587.1999.tb00577.x
Siemann E (1998). Experimental tests of effects of plant productivity and diversity on grassland arthropod diversity. Ecology 79(6):2057-2070. http://dx.doi.org/10.1890/0012-9658(1998)079[2057:ETOEOP]2.0.CO;2
Southwood TRE, Brown VK, Reader PM (1979).The relationship of plant and insect diversities in succession. Biol. J. Linn. Soc. 12:327-348. http://dx.doi.org/10.1111/j.1095-8312.1979.tb00063.x
Spanos IA, Daskalakou EN, Thanos CA (2000). Postfire, natural regeneration of *Pinus brutia* forests in Thasos Island, Greece. Acta Oecol. 21(1):13-20. http://dx.doi.org/10.1016/S1146-609X(00)00107-7
Sroka K, Finch OD (2006). Ground beetle diversity in ancient woodland remnants in north-western Germany (Coleoptera, Carabidae). J. Insect Conserv. 10:335-350. http://dx.doi.org/10.1007/s10841-006-9008-y
Sutherland WJ (2006). Ecological CensusTechniques, a handbook, 2nd edition. Cambridge UniversityPress, UK.
Tavşanoğlu Ç, Gürkan B (2014). Long-term post-fire dynamics of co-occurring woody species in *Pinus brutia* forests: The role of regeneration mode. Plant Ecol. 215:355-365. http://dx.doi.org/10.1007/s11258-014-0306-2
Thanos CA, Marcou S, Christodoulakis D, Yannitsaros A (1989). Early post-fire regeneration in *Pinus brutia* forest ecosystems of Samos island (Greece). Acta Oecol.-Oec.Plant. 10:79-94. http://users.uoa.gr/~cthanos/Papers/Samos89.pdf
Thiele HU (1977). Carabid beetles in their environments. Springer, Berlin Heidelberg, New York.
Trabaud L (2000). Post-fire regeneration of *Pinus halepensis* forests in the west Mediterranean. In Ecology, Biogeography and Managenement of *Pinus halepensis* and *Pinus brutia* Forest Ecosystems in the Mediterranean Basin edited by Ne'eman G, Trabaud L Backhuys Publishers, Leiden, The Netherlands, pp. 257-268. http://uaeco.biol.uoa.gr/files/PDF/P_G13.pdf
Trabaud L (1994). Postfire plant community dynamics in the Mediterranean basin. In The Role of Fire in Mediterranean-Type Ecosystems edited by Moreno JM, Oechel WC, Springer-Verlag, New York, pp. 1-15. http://dx.doi.org/10.1007/978-1-4613-8395-6_1
Whelan RJ (1995). The ecology of fire. Cambridge University Press, Cambridge.
Wıkars LO (2002). Dependence on fire in wood-living insects: An experiment with burned and unburned spruce and birch logs. J. Insect Conserv. 6:1-12. http://dx.doi.org/10.1023/A:1015734630309
Wikars LO, Schimmel J (2001). Immediate effects of fire-severity on soil invertebrates in cut and uncut pine forests. Forest Ecol. Manag. 141:189-200. http://dx.doi.org/10.1016/S0378-1127(00)00328-5

academicJournals

Vol. 9(19), pp. 840-843, 15 October, 2014
DOI: 10.5897/SRE2014.6012
Article Number: DB29E4548080
ISSN 1992-2248 © 2014

http://www.academicjournals.org/SRE

Scientific Research and Essays

Full Length Research Paper

Comparison of oral to intranasal administration of midazolam in children for dental surgery

Maisa A. Kamar[1]*, Ghazi S. Aldehayat[2], Basel M. Makhamreh[2] and Saba S. AlMadain[1]

[1]Department of Biopharmaceutics and Clinical Pharmacy, Faculty of Pharmacy, University of Jordan, Jordan.
[2]King Hussein medical Center, Amman, Jordan, Jordan.

Received 20 June, 2014; Accepted 26 September, 2014

The current study compares intranasal and oral midazolam for effect on sedation for patients requiring dental procedure. Eighty subjects between the ages of 5 and 12 years were received randomly either intranasal (0.2 mg/kg) or oral (0.5 mg/kg) midazolam. The observer assessed the children for sedation level at the following time points: Immediately before the drug was administered, and 20 and 30 min after drug administration. There were significant differences in sedation level among the both groups at the time of parental separation and at the time of induction. 39 (97.5%) and 40 (100%) of the forty patients who received oral midazolam were calm, drowsy or asleep at 20 and 30 min after drug administration, respectively. For patients who received intranasal midazolam, 32 (80%) and 33 (82.5%) of the forty patients were either calm or drowsy at 20 and 30 min after drug administration, respectively. None of the patients from the intranasal group was rated as 'asleep'. Oral midazolam was found to be statistically more effective in providing a better sedation level at the time of parental separation and at the time of induction than intranasal administration. Our findings indicate a tendency for oral midazolam to be more effective as a premedication in children before general anesthesia.

Key words: Preoperative, midazolam, sedation, anesthesia, pediatrics.

INTRODUCTION

The pre-anesthetic management in pediatric patients undergoing extensive dental treatment may be a challenge, particularly during parental separation and induction of anesthesia. The use of sedative premedication may help reduce the anxiety and minimizing psychological trauma related to anesthesia and surgery (Beeby and Hughes, 1980; Rosenbaum et al., 2009). MDZ is a potent, short-acting benzodiazepine sedative hypnotic, which has been used as a premedication for general anesthesia and routinely used in pediatric dentistry for dental procedures (Hartgraves Hartgraves and Primosch, 1994).

Midazolam has been used as a preoperative sedative agent via the intramuscular (Taylor et al., 1986), intranasal (Hartgraves and Primosch, 1994), oral (Hartgraves and Primosch, 1994; Cox et al., 2006), and rectal (Saint-Maurice et al., 1986) routes. The different routes of administration of midazolam (intranasal, oral, and rectal) for sedative premedication have been previously studied (Baldwa et al., 2012; Chhibber et al.,

*Corresponding author. E-mail: maaysa@gmail.com, Tel: +962 6 5355000. Fax: +962 6 5339649.

Table 1. Demographic data for the subjects.

Group	Oral	Intranasal
Age year mean (±SD)	7.12(1.713)	7.22(1.702)
Sex (M/F)	20/20	22/18
Weight kg mean (±SD)	26.75(5.633)	26.8(5.667)
Mean duration of anesthesia (min)	10	11

Table 2. Sedation score following oral and intranasal midazolam at 20 min after premedication administration.

Group	Agitated	Alert	Calm	Drowsy	Asleep
Oral midazolam (N=40)	0	1	7	32	0
Intranasal midazolam (N=40)	1	7	7	25	0

2011; Griffith et al., 1998; Lejus et al., 1997; Malinovsky et al., 1995). Studies by Kogan et al. (2002) and Yildirim et al. (2006) compared the intranasal and oral routes of administration of midazolam. The authors concluded that nasal midazolam induced sedation similar to that following oral administration of midazolam with a shorter delay of onset. Another study by Lee-Kim et al. (2004) demonstrated that the oral route of administration has higher level of sedative action and longer working time than intranasal.

The purpose of this study is to compare the effectiveness of oral and intranasal midazolam in achieving sedation in children prior to dental surgery.

MATERERIALS AND METHODS

This study's experimental protocol was approved by the local medical committee of King Hussein Medical Centre in Amman, Jordan. Informed consent was obtained from all parents of participating subjects. Eighty subjects between the ages of 5 and 12 years presenting for dental extraction under general anesthesia at King Hussein Medical Centre were included in this study between June 2013 and April 2014. All participants were in good health (ASA I). The demographic data for the children included in the study are shown in Table 1. The subjects were assigned randomly to receive either 0.5 mg/kg of oral midazolam or 0.2 mg/kg intranasal midazolam. Doses of 0.5 mg/kg for oral and 0.2 mg/kg for intranasal administration were chosen within the dose-exposure range found in preliminary studies (Acworth et al., 2001; Malinovsky et al., 1995). Half of the 80 patients received oral midazolam via a needleless syringe to the back of the mouth, whereas the other patients received intranasal midazolam as drops from a needleless syringe into the nostril.

Following drug administration, the child remained with the parent away from the treatment room for 20 min. The patient was then separated from the parent and transferred to the operatory. Vital signs were monitored continuously. Each patient was evaluated by observers for sedation level with assessments recorded immediately before the drug administration and at 20 and 30 min after drug administration.

Patient sedation was evaluated by observer using a five-point sedation scale:

1. Agitated, that is, clinging to parent and / or crying.
2. Alert, that is, a wake but not clinging to parent.
3. Calm, that is, sitting or lying comfortably with eyes spontaneously open.
4. Drowsy, that is, sitting or lying, comfortably with eyes closed but responding to minor stimulation.
5. Asleep, that is, eyes closed and not responding to minor stimulation.

The scale was devised by Wilton et al. (1988) to evaluate level of sedation of preschool children before anesthesia for surgery.

All children received a standardized GA by the same anesthesiologist. The anesthesiologist used mask induction with sevoflurane, oxygen and nitrous oxide. Thereafter, 2 g/kg of fentanyl and 0.5 mg/kg of atracurium were injected to facilitate tracheal intubation. Sevoflurane was the inhalational anesthetic used for maintenance of anesthesia. Patients' electrocardiogram, arterial blood pressure, pulse oximetry, were monitored as part of standard GA procedure following surgery, the patient was taken to the post anesthesia care unit (PACU), where the patient was monitored continuously for 1 h. The means for weight and age were analyzed using a paired t test.

Findings for sedation levels were analyzed for statistically significant differences between the groups at 20 and 30 min after midazolam administration using the Mann-Whitney U test. Mann-Whitney U test at the 95% significance level was used to compare the effectiveness of the two routes of midazolam administration. $P < 0.05$ was considered significant. The independent variable in the study was drug administration route (oral or intranasal). The dependent variable in the assessment of the effectiveness of each route was the sedation level.

RESULTS

Both groups were comparable with respect to age, weight, and duration of anesthesia as shown in Table 1. The children's reaction to being separated from their parent(s) 20 min after receiving premedication is displayed in Table 2. Changes in sedation levels following oral and intranasal midazolam at 30 min after

Table 3. Change at 30 min.

Group	Agitated	Alert	Calm	Drowsy	Asleep
Oral midazolam(N=40)	0	0	7	32	1
Intranasal midazolam(N=40)	1	6	8	25	0

Table 4. Vital signs values across procedure.

Parameters	Oral	Intranasal
HR(beat/minute)	90-128	92-120
SBP(mm hg)	70-120	80-120
DBP(mm hg)	50-70	50-80
Oxygen saturation	95-98	95-98

premedication administration are shown in Table 3.

A significant difference was observed during the 20 and 30-minute time-period between the 2 regimens: Intranasal midazolam showed more children agitated and alert, while oral midazolam presented more children quiet or asleep.

For patients who received intranasal midazolam, 32 (80 %) of the forty patients were calm, drowsy or asleep and 8 (20%) were rated as agitated, alert at 20 min, However, no significant changes in sedation scores were noted at 30 min as the number of agitated or alert participants decreased from 8 to 7 (17.5 %) while the number of calm and drowsy participants increased from 32 to 33 (82.5%). None of the patients from the intranasal group were rated as asleep.

For patients who received oral midazolam, 39 (97.5%) of the forty patients were calm, drowsy or asleep and one patient (2.5%) was rated as alert at 20 min, and none of the children in the oral midazolam group was rated as agitated or alert at 30 min. This difference was statistically significant between the group that received the oral midazolam and the group that received intranasal midazolam at the time of parental separation, $z = -1.997$ ($p = 0.046$), and at the time of induction, $z = -2.386$ ($p = 0.017$).

During the premedication time, none of the patients in the study had an incidence of bradycardia, hypotension or desaturation episodes. During the procedure time, blood pressure and pulse oximetry values for all subjects were in the normal range as shown in Table 4.

All children in the both groups recovered spontaneous ventilation. The time taken for discharge from recovery room was 28 to 50 min which was similar in both groups.

DISCUSSION

Several studies have suggested that midazolam is an effective premedication for children when administered intramuscularly (Taylor et al., 1986), rectally (Saint-Maurice et al., 1986), intranasal (Hartgraves and Primosch, 1994), or orally (Hartgraves and Primosch, 1994; Cox et al., 2006).

Studies by Kogan et al. (2002) and Yildirim et al. (2006) found that both intranasal and oral midazolam produces good levels of sedation and anxiolysis, but no significant difference in the effects of sedation was observed between the oral midazolam group and the intranasal midazolam group.

A study by Lee-Kim et al. (2004) demonstrated no statistical difference for overall behavior between the oral midazolam group and the intranasal midazolam group however intranasal subjects showed more movement and less sleep toward the end of the dental procedures, and faster onset time but shorter working time than oral midazolam group.

When assessing the level of sedation, both routs were effective but the difference in sedation level between the 2 routes of administration was significant at the time of parental separation and at the time of anesthesia.

The improvement and success in pediatric sedation over time for patients receiving oral midazolam may have been affected by the method of drug administration and the amount of drug absorption. Unlike oral administration, where its effect last for longer time, too rapid an administration via the intranasal route could result in loss of the premedication into the oral cavity. The result is less drug absorption into the nasal mucosa and, therefore, a lower blood level of the drug and a decrease in sedation with time progression.

The results of the present study must be interpreted in light of the small number of participants enrolled. Further investigation with a greater number of patients might yield more meaningful results.

The dental anesthesiologist noted that the intranasal route of midazolam administration could produce a burning sensation when the liquid is administered. Furthermore, the drug can have a noxious taste when administered via the intranasal route and more can be lost through the oronasal pathway, rendering the intranasal midazolam less effective.

Time points should be appropriate to achieve onset time of premedication. Further investigation with a greater number of time points to determine the minimum time interval between oral midazolam or intranasal midazolam premedication and separation from parents to ensure a smooth separation should be conducted.

Conclusion

Oral midazolam could be more effective as a

premedication than the intranasal route was noted in the present study. When used before general anesthesia, the oral route allowed for a better sedation level at the time of parental seperation and anesthesia than the intranasal route.

Conflict of Interest

The authors have not declared any conflict of interest.

REFERENCES

Acworth JP, Purdie D, Clark RC (2001). Intravenous ketamine plus midazolam is superior to intranasal midazolam for emergency paediatric procedural sedation. Emerg. Med. J. 18:39-45. http://dx.doi.org/10.1136/emj.18.1.39

Baldwa NM, Padvi AV, Dace NM, Garasia MB. (2012). Atomised intranasal midazolam spray as premedication in pediatric patients: comparison between two doses of 0.2 and 0.3 mg/kg. J. Anesth. 26:346-50. http://dx.doi.org/10.1007/s00540-012-1341-6

Beeby DG, Hughes JOM (1980). Behaviour of unsedated children in the anaesthetic room. Br J Anaesth. 52:279-281. http://dx.doi.org/10.1093/bja/52.3.279

Chhibber AK, Fickling K, Lustik SJ (2011). Pre-Anesthetic Midazolam: A Randomized Trial with three Different Routes of Administration. J. Anesth. Clin. Res. 2:118. http://dx.doi.org/10.4172/2155-6148.1000118

Cox RG, Nemish U, Ewen A, Crowe MJ (2006). Evidence-based clinical update: Does premedication with oral midazolam lead to improved behavioral outcomes in children. Canad. J. Anesth. 53(12):1213-1219. http://dx.doi.org/10.1007/BF03021583

Griffith N, Howell S, Mason DG (1998). Intranasal midazolam for premedication of children undergoing day-case anaesthesia: comparison of two delivery systems with assessment of intra-observer variability. Br. J. Anaesth. 81(6):865-869. http://dx.doi.org/10.1093/bja/81.6.865

Hartgraves PM, Primosch RE (1994). An evaluation of oral and nasal midazolam for pediatric dental sedation. J. Dent Child. pp. 61175-61181.

Kogan A, Katz J, Efrat R, Eidelman LA (2002). Premedication with midazolam in young children: A comparison of four routes of administration. Paediatr Anaesth. 12:685-689. http://dx.doi.org/10.1046/j.1460-9592.2002.00918.x

Lee-Kim SJ, Fadavi S, Punwani I, Koerber A (2004). Nasal versus oral midazolam sedation for pediatric dental patients. J. Dent. Child. 71:126-130.

Lejus C, Renaudin M, Testa S, Malinovsky JM, Vigier T, Souron R (1997). Midazolam for premedication in children: nasal vs. rectal administration. Eur. J. Anaesthesiol. 14:244-249. http://dx.doi.org/10.1097/00003643-199705000-00004

Malinovsky JM, Populaire C, Cozian A, Lepage JY, Lejus C, Pinaud M (1995). Premedication with midazolam in children: effect of intranasal, rectal and oral routes on plasma midazolam concentration. Anaesthesia. 50:351-354. http://dx.doi.org/10.1111/j.1365-2044.1995.tb04616.x

Rosenbaum A, Kain ZN, Larsson P, Lönnqvist PA, Wolf AR (2009). The place of premedication in pediatric practice. Paediatr. Anaesth. 19(9):817-828. http://dx.doi.org/10.1111/j.1460-9592.2009.03114.x

Saint-Maurice C, Meistleman C, Rey E, Esteve C, De Lauture D, Olive G (1986). The pharmacokinetics of rectal midazolam for premedication in children. Anesthesiol. 65:536-538. http://dx.doi.org/10.1097/00000542-198611000-00019

Taylor MB, Vine PR, Hatch DJ (1986). Intramascular midazolam premedication in small children. Anaesth. 41:21-26. http://dx.doi.org/10.1111/j.1365-2044.1986.tb12698.x

Wilton NCT, Leigh J, Rosen DR, Pandit UA (1988). Preanesthetic sedation of preschool children using intranasal midazolam. Anesthesiol. 69:972-975. http://dx.doi.org/10.1097/00000542-198812000-00032

Yildirim SV, Guc BU, Bozdogan N, Tokel K (2006). Oral versus intranasal midazolam premedication for infants during echocardiographic study. Adv. Therapy 23:719-724. http://dx.doi.org/10.1007/BF02850311

academicJournals

Vol. 9(19), pp. 844-850, 15 October, 2014
DOI: 10.5897/SRE2014.6050
Article Number: E43A12648082
ISSN 1992-2248 © 2014

http://www.academicjournals.org/SRE

Scientific Research and Essays

Full Length Research Paper

Evaluation for nutritive values and antioxidant activities of Bang Chang's Cayenne pepper (*Capsicum annuum* var. *acuminatum*)

Yuttana Sudjaroen

Faculty of Science and Technology, Suan Sunandha Rajabhat University, Bangkok, 10300 Thailand.

Received 24 July, 2014; Accepted 3 October, 2014

This objectives of this study were evaluated nutritive values of Bang Chang's Cayenne pepper (*Capsicum annuum* var. *acuminatum*) and investigates its biological characteristics on health promotion, such as, antioxidant activities. The research was conducted by collecting sample, separating dried edible parts, which were determined nutritive values, including proximal analysis of water content, crude protein, crude fat, dietary fiber, total ash content, carbohydrate, total calories, β-carotene, vitamins E and C. The nutritive data show higher nutritive values of Bang Chang's Cayenne pepper than other Cayenne pepper. Moreover, β-carotene and vitamin E contents of Bang Chang's Cayenne pepper were higher than other Cayenne pepper. In conclusion, Bang Chang's Cayenne pepper was quite more good nutritive values than other Cayenne peppers with preferable antioxidant activities and non-toxic effect on Vero cell.

Key words: Bang Chang's Cayenne pepper, *Capsicum annuum* var. *acuminatum*, nutritive value, antioxidant activity, cytotoxicity.

INTRODUCTION

Capsicum annuum in Solanaceae genus is a non-pungent pepper, which is important ingredients in many traditional dishes as decorative vegetables due to their colors (such as green red and yellow) and unique taste. Peppers are found to be sources of bioactive compounds such as vitamin C, vitamin E, provitamin A, carotenoids, phenolics and flavonoids (Materska and Perucka, 2005) with antioxidant activities, which promote reduction of harmful oxidative stress. These compounds could also prevent many diseases that related with free radical oxidation such as cardiovascular disease, cancer and neurological disorders (Shetty and Wahlqvist, 2004). According to various appearances of sweet peppers, relationship between different color sweet peppers and antioxidant activities is of interesting topic. The sweet peppers with difference colors may compose of diverse pigment generators. Carotenoids (including capsanthin, capsorubin and capsanthin) and flavonoids are main pigment compounds in red pepper (Luke, 2000; Sun et al., 2007), while the color of green pepper is from chlorophyll and the carotenoids typical of the chloroplast (Marin et al., 2004). Likewise, yellow sweet pepper

E-mail: yuttana.su@ssru.ac.th, reefandyut@yahoo.com, Tel: (66)-2-160-1143-5. Fax: (66)-2-160-1146.

consists of α- and β-carotene, zeaxanthin, lutein and β-cryptoxanthin as color generators (Luke, 2000).

Bang Chang's Cayenne pepper (*C. annuum* var. *acuminatum*) or Bang Chang cultivar is originated from Bang Chang sub-district, Amphawa district, SamutSongkhram province, Thailand and had special characteristic for cooking, such as attractive red color or vermillion, aromatic odor after dried, appropriate to cooking and dressing to Thai cuisine.

The aim of this research was to investigate nutritive values, the total phenolic content (TPC) and antioxidant activities from dried pepper extracted in different solvent systems including hexane and ethanol. This research would provide information on the relationship between sweet peppers extracted with different solvent systems and their antioxidant activities, which could be useful for further investigation on isolation of anti-oxidative agents from Bang Chang's Cayenne peppers.

MATERIALS AND METHODS

Sample collection and preparation

The basis data of Bang Chang's Cayenne peppers, such as, cultivated area, last annual yield of production and local expert's interview, were supported by Samut Songkram agricultural extension office. The pepper harvest was done during March to April, 2014 which started to sundry during 2 to 3 days. For other, Cayenne peppers were purchased from local market of Bangkok area, which were the "mixture" of common Cayenne pepper cultivars in Thailand including "Phrik-Mun", "Phrik Chi-Fah", "Phrik-Jinda" cultivars. All samples were dried in constant weigh and selected edible parts were ground prior to evaluation of nutritive values and biological assays. All assays were carried out in triplicate and the results were described as mean values and standard deviation.

Evaluation of the nutritive values

Proximate analysis

The proximate analysis was carried out according to the methods to be described, or based on the official methods of analysis of AOAC International, 16th ed (AOAC, 1995). The fresh samples were used for the water content determination. The remaining samples were dried at 105°C for 3 h, ground, and then stored in air-tight containers in a cool, dry place for other analyses.

Water content determination

Three to five grams (3 to 5 g) of each sample was dried at 105°C for 3 h. The dried sample was then weighed. The water content was calculated as the percentage on the wet weight basis.

Determination of crude protein

Crude protein was determined by Kjeldahl method (AOAC, 1995), using Buchi Digestion Unit (B-435) and Distillation Unit (B-323) (Buchi, Switzerland). Dried sample (0.2 g) was digested with 20 ml of conc.H_2SO_4, using 3 g of the selenium and copper sulfate mixture as the catalyst. The digestion was continued for half an hour after the digestion mixture turned clear green. Then 60 ml of 32% sodium hydroxide solution was added, and the mixture was distilled for 3 min. The distillate was collected in a flask containing 60 ml of 2% boric acid solution, with methylene blue and methyl red as the indicators. The distillate was then titrated with 0.1 N H_2SO_4 solution; the end point was purple. Crude protein was calculated as the percentage on the wet weight basis (N × 6.25).

Determination of crude fat

One gram (1 g) of the dried sample was extracted with 25 ml of petroleum ether in a Goldfisch apparatus (Labconco, U.S.A.) for 3 to 4 h. The petroleum ether extract was evaporated to dryness at 105°C. The residue was weighed and then calculated as the percentage of crude fat on the wet weight basis.

Determination of dietary fiber

Insoluble dietary fiber content was determined according to the AOAC official method 991.42 (AOAC, 1995). Amyloglucosidase (conc.) in the amount of 0.1 ml was used instead of 0.3 ml of the normal strength enzyme. Soluble dietary fiber content was determined according to the AOAC official method by modified as in insoluble dietary fiber determination. The sum of both values was recorded as the total dietary fiber content of each sample.

Determination of total ash content

One gram (1 g) of each sample was ignited in a muffle furnace at 525°C until ash was obtained. The residue was weighed and expressed as total ash on the wet weight basis.

Determination of carbohydrate

The carbohydrate content was obtained by difference, subtracting the water content, crude protein, crude fat, total dietary fiber, and total ash contents from 100% w/w.

Determination of β-carotene, vitamins E and C

a) Measure β-carotene was applied from the method of Munzuroglu et al. (2003). Sample (50 g) was mashed in a homogenizer and 2 g homogenate paste per sample was taken for extraction of β-carotene. To the above homogenates, 4 ml of ethanol were added, vortexed and the mixture centrifuged (Mistral© 2000) at 2000 rpm for 3 min at 4°C. The supernatant was also filtered through a Whatman No.1 paper, and to the filtrate 0.15 ml n-hexane was added and mixed. β-Carotene was extracted twice in the hexane phase and the collected extract was dried under a stream of liquid nitrogen. Dried extract was solubilized in 0.2 ml methanol for high-performance liquid chromatography (HPLC). Injections were made in duplicate for each sample. The quantification utilized absorption spectra of 436 nm for β-carotene. HPLC separations were accomplished at room temperature with a Perkin-Elmer liquid chromatograph system (Series 1100), consisting of a sample injection valve (Cotati 7125) with a 20 ml sample loop, an ultraviolet (UV) spectrophotometric detector (Cecil 68174), integrator (HP 3395) and a Techsphere ODS-2 packed (5 mm particle and 80 A° pore size) column (250_4.6 i.d.) with a methanol: acetonitrile: chloroform (47:42:11, v/v) mobile phase at 1 ml/min flow rate.

b) Measure vitamin E was applied from the method of Qian et al.

(1998). An initial extraction procedure was developed as follows: Sample was ground in a warring blender and screened through an 80 mesh sieve. One gram (1 g) of the sample was precisely weighed and transferred to a 10-ml screw-capped extraction tube. 4ml of *n*-hexane was added to the tube and the tube was flushed with a steam of N_2 to protect vitamins from air exposure before capping. The mixture was shaken on a vortex mixer for 0.5 min, rested for 5 min, and shaken another half minute. After centrifugation at 4000 rpm for 5 min, 1 ml of supernatant was transferred to a 1.5-ml vial and evaporated under nitrogen to remove the solvent. The residue was re-dissolved in 0.3 ml *n*-butanol before being injected into the HPLC system.

Chromatographic separations were performed on a 150 × 3.9 mm Novapak C column (Waters). Methanol was used as mobile phase at a flow-rate of 1.5 ml/min and a pressure of 1000 p.s.i. (1 p.s.i. = 6894.76 Pa) All injections were 50 ml loop injections on a M710B autosampler (Waters). A Model M510 Waters pump and a Model M490 Waters variable Wavelength UV-visible detector set at 290 nm were used. All quantitation was by peak area using a Waters M740 integrator. Based on the established chromatographic conditions, repeated injections of 0.1, 0.5, 1, 5 and 10 mg of the standard vitamin E was made duplicated onto the HPLC system. The retention time for vitamins E was 4.1 min. A Shimadzu MPS-2000 universal spectrophotometric scanner was used to determine the spectrograms of vitamin E in *n*-butanol.

c) Measure vitamin C was applied from the method of Sanchez-Moreno et al. (2003). Total vitamin C (ascorbic acid plus dehydroascorbic acid) were determined by HPLC. The procedure employed to determine total vitamin C was the reduction of dehydroascorbic acid to ascorbic acid, using DL-dithiothreitol as reductant reagent. A volume of 50 ml of each orange juice was homogenized with 40 ml of an extraction solution (3% metaphosphoric acid plus 8% acetic acid). The resulting mixture was centrifuged, filtered, and adjusted to 100 ml with distilled water. Samples were filtered through a 0.45 µm membrane filter, and duplicates of 20 µl for each extract were analyzed by HPLC. Results were expressed as milligrams of ascorbic acid per 100 ml. An aliquot of the mixture was taken to react with 2.0 ml of a solution 20 mg/ml DL-dithiothreitol for 2 h at room temperature and in darkness. During this time the reduction of dehydroascorbic acid to ascorbic acid has been placed. Samples were filtered through a 0.45-µm membrane filter, and duplicates of 20 µl for each extract were analyzed by HPLC. Results were expressed as milligrams of total vitamin C per 100 ml. A Hewlett-Packard model 1050 quaternary solvent delivery controller pump was used for analysis. Samples was introduced onto the column via a manual injector (Rheodyne) equipped with a sample loop (20 µl). Separation of ascorbic acid was performed by HPLC using a reversed-phase C18 Hypersil ODS (5 µm) stainless steel column (250 × 4.6 i.d. mm) (Technochroma). The solvent system used was an isocratic gradient of a 0.01% solution of H_2SO_4, adjusted to pH 2.5 to 2.6. The flow rate was fixed at 1.0 ml/min. A Hewlett-Packard 1040A UV-visible photodiode array detector was set at 245 nm; chromatographic data and UV-visible spectra were collected, stored, and integrated using a Hewlett-Packard Chem Station and related software. Identification of the ascorbic acid was carried out by HPLC by comparing the retention time and UV-visible absorption spectrum with those of the standard previously referred to. Calibration curves were built with a minimum of four concentration levels of ascorbic acid standard.

Test of biological activities

The pepper samples were dried by hot air and ground. Bring 100 g of ground dried pepper for continuous extraction, then, extract with hexane and ethanol using Soxhlet apparatus. Finally, get the solvent evaporated through rotary evaporation apparatus under vacuum.

Total phenolic content (TPC)

Measurement using Folin-Ciocalteu reagent (Singleton et al., 1999) was done by comparing it with standard solvent, that is, gallic acid at 1 to 0.125 mg/ml concentration; then, calculating TPC of gallic acid in mg/g of the extracts.

Antioxidant activity measurement

a) 2,2-Diphenylpicrylhydrazyl (DPPH) radical scavenging assay to measure the decreasing light absorbance of DPPH radical (Yen and Duh, 1994) using negative control by DPPH radical (6×10^{-5} M), promptly measure at nm and positive control using vitamin C.

b) 2, 2-Azinobis (3-ethyl-benzothiazoline-6-sulfonic acid) (ABTS) cation radical scavenging assay similar to the 1st method but using ABTS radical instead (Re et al., 1999) and also using Trolox (soluble vitamin E) as standard substance to create standard graph (0.5 to 5.0 mg/ml concentration). The antioxidant activity of the Bang Chang's Cayenne peppers would be shown in Trolox equivalent antioxidant capacity (TEAC)/gm of the pepper extracts.

c) Oxygen radical absorbance capacity (ORAC) to measure ability of extract to scavenge oxygen radical (Prior et al., 2003) and the fluorescent signal generated by fluorescene sodium salt (Sigma-aldrich, Inc.) was measured by FLUOstar OPTIMA microplate reader (BMG) for 1 h. The antioxidant activity of the Bang Chang's Cayenne peppers would be also shown in TEAC/gm of the pepper extracts.

Cytotoxic activity screening test

Test for cytotoxic activity on primate cell line (Vero cell) using green fluorescent protein (GFP)-based assay (Hunt et al., 1999) by ellipticine as a positive control and 0.5% dimethyl sulfoxide (DMSO) as a negative control.

RESULTS

Nutritional value of Bang Chang's Cayenne peppers

It was found that there were higher nutritive values of Bang Chang's Cayenne pepper than other Cayenne pepper including β-carotene, vitamins E and C as shown in Table 1. Both samples were lack of vitamin C contained that may be affected by sundried preparation.

Biological properties of Bang Chang's Cayenne peppers

As a result, it was found that Bang Chang's Cayenne pepper extracted with ethanol exhibited the higher TPC and antioxidant activities than hexane extract (TPC of 256.4 ± 18.9 mg GAE/100 g, DPPH values of 1751.8 ± 119.1 µmole TEAC/100 g, $ABTS^{+\cdot}$ values of 2663.2 ± 79.0 µmole TEAC/100 g and ORAC values of 4166.3 ± 103.8 µmole TEAC/100 g), followed (Table 2). The test

Table 1. Nutritive values of Bang Chang's Cayenne pepper and other Cayenne peppers*.

Variable	Bang Chang'sCayenne pepper	OtherCayenne peppers**
Water (%w/w)	98.5	97.3
Crude protein (%w/w)	3.2	2.7
Crude fat (%w/w)	1.3	0.8
Total ash (%w/w)	1.6	1.1
Dietary fiber (%w/w)	3.8	3.2
Carbohydrate (%w/w)	9.1	6.8
Total calories (Kcal/100 g)	103	101
β-carotene (µg/100 g)	1,418	1.235
Vitamin E (mg/100 g)	48.68	32.86
Vitamin C (mg/100 g)	-	-

*Data are expressed as means of triplicate; ** The "mixture" of common Cayenne pepper cultivars in Thailand including "Phrik-Mun", "Phrik Chi-Fah", "Phrik-Jinda" cultivars.

Table 2. Total phenolic content (TPC) and free radical scavenging activities of hexane and ethanol extracts from Bang Chang's Cayenne pepper*.

Study/References		TPC	DPPH·	$ABTS^{+\cdot}$	ORAC	β-Carotene bleaching test (60 min)	Fe^{2+} chelating activity
C. annum on this study							
Bang Chang cultivar:	Hexane	1.1 ± 0.1[1]	61.0 ± 2.6[2]	45.4 ± 2.4[2]	198.6 ± 7.8[2]	-	-
	Ethanol	256.4 ± 18.9[1]	1751.8 ± 119.1[2]	2663.2 ± 79.0[2]	4166.3 ± 103.8[2]	-	-
C. annum (Loizzo et al., 2013)							
Roggiano cultivar	Hexane	-	55.1 ±1.9[3]	52.1 ± 1.9[2]	-	178.0 l [3]	189.1 l [3]
	Ethanol	-	186.4 ± 3.4[3]	181.4 ± 3.4[2]	-	155.6 l [3]	131.4 ± 2.8[3]
Senise cultivar	Hexane	-	52.1 ± 1.9[3]	21.4 ± 1.5[2]	-	298.6 ± 3.9[3]	90.4 ± 3.8[3]
	Ethanol	-	81.4 ± 3.4[3]	12.6 ± 1.1[2]	-	63.6 ± 1.8[3]	153.7 ± 4.4[3]
C. annum: (Hernández et al., 2010)							
Extractable and hydrolysable polyphenols	Arbol cultivar	-	-	38.5 ± 0.4[4]	-	-	82.3 ± 1.3[4]
	Chipotle cultivar	-	-	44.4 ± 0.6[4]	-	-	80.6 ±1.2[4]
	Guajillo cultivar	-	-	26.6 ± 1.0[4]	-	-	63.9 ± 0.9[4]
	Morita cultivar	-	-	35.0 ± 0.5[4]	-	-	73.9 ± 0.9[4]

[1]mg GAE/100 g DW; [2]µmole TEAC/100 g DW; [3]50% of inhibitory concentration (IC_{50}); [4]µ0% e TEAC/g of polyphenols. GAE = Gallic acid equivalent, TEAC = Trolox equivalent antioxidant capacity, DW = dried weight.

Table 3. Cytotoxic effect of Bang Chang's Cayenne pepper extracts to Vero cells.

Extract	Final conc. (µg/ml)	% Growth	Cytotoxicity
Hexane	50.0	75.60	Non-cytotoxic
	25.0	85.11	Non-cytotoxic
	12.5	92.24	Non-cytotoxic
	6.25	97.16	Non-cytotoxic
	3.125	98.11	Non-cytotoxic
	1.5625	99.79	Non-cytotoxic
	0.7813	99.31	Non-cytotoxic
Ethanol	50.0	90.13	Non-cytotoxic
	25.0	93.79	Non-cytotoxic
	12.5	94.04	Non-cytotoxic
	6.25	96.82	Non-cytotoxic
	3.125	100.00	Non-cytotoxic
	1.5625	100.00	Non-cytotoxic
	0.7813	100.00	Non-cytotoxic

Figure 1. Fresh Bang Chang's Cayenne pepper (left) and after dried (right).

for the cytotoxic activity on cell showed that hexane and ethanol extract yielded no toxic on Vero cell at the concentration of 50 µg/ml (Table 3). The antioxidant activity values from all methods were related to amount of phenolic content.

DISCUSSION

These results corresponded to the previous research (Sun et al., 2007), which found that methanol could extract higher quantity of flavonoids such as quercetin and luteolin from red pepper (Sun et al., 2007). Our ethanol extract had higher polarity, however, its polarity closed to methanol, thus ethanol extract may contain high amount of phenolic compounds that correlated to TPC as well. Additionally, red pepper was also reported to contain higher quantity of flavonoids than green pepper (Materska and Perucka, 2005) and when compared to our study, Bang Chang's Cayenne pepper had attractive red color (Figure 1), which may also contain high amount of flavonoids. On the previous studies, Loizzo et al (2014) were evaluated antioxidant activities of *C. annum* (two cultivars) by wide range methods (Table 2) including $DPPH^{\cdot}$, $ABTS^{+\cdot}$, β-carotene bleaching test and Fe^{2+} chelating activity test. Ethanol extract of Bang Chang's Cayenne pepper was possessed $ABTS^{+\cdot}$ radical scavenging values higher than all extracts (Table 2) from previous study (Loizzo et al., 2014; Hernández et al., 2010). It may also have higher antioxidant activity than Cayenne peppers on previous studies according to $DPPH^{\cdot}$ radical scavenging assay, however, incomparable for $DPPH^{\cdot}$ radical scavenging assay, because of different on reported value (between µmole TEAC/100 g DW and 50% of inhibitory concentration, IC_{50}). Moreover, antioxidant activities of Cayenne peppers were preferable on other antioxidant assay also (Loizzo et al., 2014; Hernández et al., 2010) and different on temperatures

and assays may affect antioxidant values (Yazdizadeh et al., 2013).

These results suggested that TPC and antioxidative agents might possess hydrophilic properties more than lipophilic properties, and were corresponded to the previous research, which reported that flavonoids are commonly extracted with methanol or ethanol solvent systems (Bae et al., 2012). Bang Chang's Cayenne pepper contained higher nutritive values rather than other Cayenne pepper, because amount of fleshy pulp was thicker than other Cayenne pepper when compared in the same weight and ease to ground for cooking as spices. Polyphenolic compounds may have the major bioactive components in Bang Chang's Cayenne pepper, which are responsible for antioxidation and antiproliferation. Natural antioxidants have been proved to inhibit tumor growth selectively, because of different redox status between normal cells and cancer cell (Nair et al., 2007). In case of this study, both of extracts lack cytotoxicity against a noncancerous cell line, Vero cells and this results was corresponded to previous study, which was reported to lack of cytotoxicity on *C. annum* against Vero cell line and an adenocarcinoma cervical cancer, HeLa cell line study (Berrington and Lall, 2012). However, *C. annum* was exhibited cytotoxicity against hepatocellular cancer cell, Hep-G2 cell line and the cytotoxicity of pepper was depended on red color peppers with small size and capsaicin content (Popovich et al., 2014).

Conclusion

The nutritional values of Bang Chang's Cayenne pepper were higher than other Cayenne pepper and may contain antioxidant substances with non-toxic property. These pepper provided the highest antioxidant activity in hydrophilic extract because of higher TPC and antioxidant activity in ethanol extract, which is suggesting that bioactive compounds are well soluble in hydrophilic solvent. This research will be useful for further investigation on isolation of anti-oxidative agents from Bang Chang's Cayenne pepper.

Conflict of Interest

The author(s) have not declared any conflict of interest

ACKNOWLEDGEMENTS

The researcher would like to express their gratitude to Research and Development Institute of Suan Sunandha Rajabhat University, Bangkok, Thailand for the funding support. I am grateful to Faculty of Science and Technology, Saun Sunandha Rajabhat University, National Center for Genetic Engineering and Biotechnology for research facility support.

I would like to sincerely thank all staff and the students of Home Economics, Faculty of Science and Technology for the support on the information of Bang Chang's Cayenne pepper for Thai cuisine.

REFERENCES

AOAC (1995). Official Methods of Analysis of AOAC International. Vol. II. 16th ed. Alington: AOAC International.

Berrington D, Lall N (2012). Anticancer activity of certain herbs and spices on the cervical epithelial carcinoma (HeLa) Cell Line. Evid. Based Complement Alternat. Med. Volume 2012:11 pages.

Hernández D, Sáyago-Ayerdi SG, Go-i I (2010). Bioactive compounds of four hot pepper varieties (Capsicum annuum L.), antioxidant capacity, and intestinal bioaccessibility. J. Agric. Food Chem. 58(6): 3399-3406. http://dx.doi.org/10.1021/jf904220w

Hunt L, Jordan M, De Jesus M, Wurm MF (1999). GFP-expressing mammalian cells for fast, sensitive, noninvasive cell growth assessment in a kinetic mode. Biotechnol. Bioeng. 65(2):201-205. http://dx.doi.org/10.1002/(SICI)1097-0290(19991020)65:2<201::AID-BIT10>3.0.CO;2-H

Loizzo MR, Pugliese A, Bonesi M, De Luca D, O'Brien N, Menichini F, Tundis R (2014). Influence of drying and cooking process on the phytochemical content, antioxidant and hypoglycaemic properties of two bell Capsicum annum L. cultivars. Food Chem. Toxicol. 53:392-401. http://dx.doi.org/10.1016/j.fct.2012.12.011

Luke RH (2000). Antioxidant vitamin and phytochemical content of fresh and processed pepper Fruit (Capsicum annuum), Handbook of Nutraceuticals and Functional Foods, CRC Press, USA.

Marin A, Ferreres F, Tomas-Barberan FA, Gil MI (2004). Characterization and quantitation of antioxidant constituents of sweet pepper (Capsicum annuumL.). J. Agric. Food Chem. 52(12): 3861-3869. http://dx.doi.org/10.1021/jf0497915

Materska M, Perucka I (2005). Antioxidant activity of the main phenolic compounds isolated from hot pepper fruit (Capsicum annuumL), J. Agric. Food Chem. 53(5):1750-1756. http://dx.doi.org/10.1021/jf035331k

Munzuroglu O, Karatas F, Geckil H (2003). The vitamin and selenium contents of apricot fruit of different varieties cultivated in different geographical regions. Food Chem. 83:205-212. http://dx.doi.org/10.1016/S0308-8146(03)00064-5

Nair S, Li W, Kong AT (2007). Natural dietary anti-cancer chemopreventive compounds: Redox-mediated differential signaling mechanisms in cytoprotection of normal cells versus cytotoxicity in tumor cells. Acta Pharmacol.Sin. 28(4):459-472. http://dx.doi.org/10.1111/j.1745-7254.2007.00549.x

Qian H, Sheng, M (1998). Simultaneous determination of fat-soluble vitamins A, D and E andpro-vitamin D2 in animal feeds by one-step extraction and high-performance liquid chromatography analysis. J. Chromatogr. A. 825:127-133. http://dx.doi.org/10.1016/S0021-9673(98)00733-X

Popovich DG, Sia SY, Zhang W, Lim ML (2014). The color and size of chili peppers (Capsicum annuum) influence Hep-G2 cell growth. Int. J. Food Sci. Nutr. 24:1-5. http://dx.doi.org/10.3109/09637486.2014.931358

Prior RL, Hoang H, Gu L, Wu X, Bacchiocca M, Howard L, Hampsch-Woodill M, Huang D, Ou B, Jacob R (2003). Assays for hydrophilic and lipophilic antioxidant capacity (Oxygen radical absorbance capacity (ORACFL) of plasma and otherbiological and food samples. J. Agric. Food Chem. 51(11):3273-3279. http://dx.doi.org/10.1021/jf0262256

Re R, Pellegrini N, Proteggente A, Pannala A, Yang M, Rice-Evans C (1999). Antioxidant activity applying an improved ABTS radical cation decolorization assay. Free Radic. Biol. Med. 26(9-10):1231-1237. http://dx.doi.org/10.1016/S0891-5849(98)00315-3

Sanchez-Monreno C, PlazaL, de Ancos B, Cano MP (2003). Vitamin C, provitamin A carotenoids, and other carotenoids in high-pressurized orange juice during refrigerated storage. J. Agric. Food Chem. 51(3): 647-653. http://dx.doi.org/10.1021/jf020795o

Shetty K, Wahlqvist ML (2004). A model for the role of the proline-linked pentose-phosphate pathway in phenolic phytochemical bio-synthesis and mechanism of action for human health and environmental applications. Asia. Pac. J. Clin. Nutri. 13(1):1-24.

Singleton LV, Orthofer R, Lamuela-Raventós MR (1999).Analysis of total phenols and other oxidation substrates and antioxidants by means of Folin-ciocalteu reagent. Methods Enzymol. 299:152-178. http://dx.doi.org/10.1016/S0076-6879(99)99017-1

Sun T, Xu Z, Wu CT, Janes M, Prinyawiwatkul W, No HK (2007). Antioxidant activities of different colored sweet bell peppers (Capsicum annuum L.). J. Food Sci. 72(2):98-102. http://dx.doi.org/10.1111/j.1750-3841.2006.00245.x

Yazdizadeh NS, Jamei R, Heidari R (2013). Antioxidant activities of two sweet pepper Capsicum annuum L. varieties phenolic extracts and the effects of thermal treatment. Avicenna J. Phytomed. Winter. 3(1):25-34.

Yen CG, Duh DP (1994). Scavenging effect of methanolic extracts of Peanut hulls on free-radical and active-oxygen species. J. Agric. Food Chem. 42(3):629-632. http://dx.doi.org/10.1021/jf00039a005

academicJournals

Vol. 9(19), pp. 851-863, 15 October, 2014
DOI: 10.5897/SRE2014.5987
Article Number: DC05CA748085
ISSN 1992-2248 © 2014

http://www.academicjournals.org/SRE

Scientific Research and Essays

Full Length Research Paper

Numerical simulation of rainfall-induced rock mass collapse and debris flow

Jikun Zhao[1,2]*, Dan Wang[1], Daming Zhang[3] and Huiqing Zhang[1]

[1]College of Engineering, Nanjing Agricultural University, Nanjing 210031, China.
[2]Jiangsu Key Laboratory for Intelligent Agricultural Equipment, Nanjing 210031, China.
[3]Department of Industrial Technology, California State University, Fresno 93740, Amercica.

Received 28 May, 2014; Accepted 26 September, 2014

Geologic disaster of rainfall-induced rock collapse and debris flow is an essential part of research in the field of geotechnical engineering. Based on the discrete element method, the article derived the constitutive model of particles bond-damage fracture-move. A two-dimensional slope model of rock mass collapse was established to simulate slide of rock mass collapse and dynamic evolution process of debris flow. The change of mechanics parameters of six monitoring points were tracked and analyzed. The results showed that, nonlinear motion of microscopic particles was obvious during the process of bond-damage fracture-move. Based on the geological conditions of rock mass collapse and debris flow on Greenland in Denmark, a three-dimensional slope model was established. The results showed displacements and velocities of measuring points both displayed linear relationship with slope when slope increased from 1.0 to 2.0; while non-linear capacity was strong under the slope with a degree above 2.0. The research will be the foundation for nonlinear movement of debris flow and this kind of disaster induced by different factors.

Key words: Discrete element method, rock mass collapse, microscopic failure, debris flow, numerical simulation.

INTRODUCTION

Slope sliding and debris flow is a typical geological disaster whose forming mechanism is influenced by many factors. As movements of geological disasters induced by rainfall are complex, some technical problems have not been broken through on dynamic problems. Researches on dynamics of debris flow are currently hot and difficult problems for academia.

In order to explore the physical mechanism of debris flow, scholars at home and abroad have done much research on theoretical exploration and practical application (Iverson, 1997; Kane and Ponten, 2012; Neal et al., 2013). As a kind of special fluid, debris flow possesses of tremendously complex features. Scholars mainly establish dynamic model of debris flow basing on the theory of SH and their researches on processes of debris flow always focus on numerical simulation (Tang, 1994; Yu, 1996; Ma et al., 2008). The United States Geological Survey (USGS) set up the institutions on debris flow and their statistical model has been applied. Many scholars in the domestic such as Du (1987), Wu (1990), Kang (2004) and so on, have made pioneering research on formation mechanism of debris flow in China

*Corresponding author. E-mail: jikunzhao_2006@163.com, Tel: +8613675132073. Fax: +862558606573.

and accumulated valuable observation data.

Gravity is the main driving force of rainfall inducing rock collapse and debris flow. The dynamic mechanism of liquid is very complicated that contains many forms of motion, such as collision, friction, sliding and rotation between particles. An important approach to studying its movement is numerical calculation. Discrete element method has been utilized in many researches for slope stability (Federicoa and Michaele, 2007; Lei and Wang, 2006). It also has a big superiority in solving the formation and evolution process of debris flow and has solved the difficult problem on movement evolution of discontinuous medium. Sitharam and Vinod (2010) attained the degree of impact of other factors on dynamic shear modulus and damping ratio of particle materials through Discrete Element Method (DEM). Mohsin et al. (2013) established a one-dimensional model by using Hydrologic Engineering Center River Analysis System (HEC-RAS) and studied debris flow in view of dam break. Wang and Fulvio (2011) analyzed the influence of factors on rock collapse by DEM. The parametric inversion analysis on the rolling motion was completed by Jiang et al. (2008) through DEM. Li et al. (2009) analyzed stability of rock slope by DEM. Tang and Xu (2007) studied problems on geotechnical multi-scale by coupling the discrete element and shell finite element. Zhou et al. (2010) realized the two dimensional discrete-continuous coupling analysis for problems on geotechnical engineering deformation by Particle Flow Code (PFC) and Fast Lagrangian Analysis of Continua (FLAC) Socket I/O interface; numerical examples showed the effectiveness of the method on coupling analysis. Fan et al. (2010) simulated dynamic process of entrainment along the way, they found that the entrainment action could increase the motion volume of debris flow and the debris flow would be more destructive and harmful. Based on the Bingham theological theory, Zhang et al. (2012) built a model of debris flow, simulated the gully bed evolution and carried out the bed erosion-deposition processes. Nicholas et al. (2014) analyzed seven debris flows initiated in proglacial gullies. The high slopes and elevations of debris flow-producing proglacial areas reflect positive slope-elevation trends for the Mount Rainier volcano.

Rock collapse is a key cause secondary disaster. Such as sediment deposition, debris flow erosion, impact and stacking problems. Erosion and the impact of disasters is one of the main causes of the disaster along the way. Sediment deposition is one of the main causes of the local lake. Because of the above reasons, the paper studied rock collapse and sediment deposition. Research on effects of microscopic mechanic parameters on the macroscopic characteristics in process of rock mass collapse and debris flow is less. Based on the discrete element method, the article derived the constitutive model of particles connect-damage fracture-move. A slope model was established to simulate slide of rock mass collapse and dynamic process of debris flow. The article also analyzed mechanism characteristics of rock collapse and evolution of debris flow under different slopes.

THE CONSTITUTIVE MODEL OF PARTICLES BOND-DAMAGE FRACTURE-MOVE

There are two kinds of connected models on discrete element. One is contact connection model which is equal to the rigid ring joint at contact points; there is a pair of springs with a constant normal stiffness and the tangential stiffness which can only transmit force. It cannot transmit bending moment; otherwise it will break when the force is greater than the connection strength. The other is parallel connection model which is equal to the flexible rubber connection on the contact surface and has rigidity connection itself. It will fracture when the force is greater than the connection strength. However, it cannot describe the particle damage stage. The paper deduced the constitutive model of damage of the particle. Microscopic parameter of contact connection model consists of normal connection strength and tangential connection strength. Zhao et al. (2013) have derived constitutive model of particles bond-damage fracture before. The paper would derive the equation of movement after the particles being damaged.

Assume that A and B are two adjacent particles of rock mass and the connection damage mechanical behavior is described by normal connection strength; tangential connection strength; normal connection stiffness; tangential connection stiffness and connection radius. The unit normal vector n_i of particle - particle interface is represented as:

$$n_i = \frac{x_i^{[B]} - x_i^{[A]}}{d} \tag{1}$$

In the formula, $x_i^{[A]}$ and $x_i^{[B]}$ are the center vector of particles A and B, respectively; center distance d between particles is:

$$d = \left| x_i^{[B]} - x_i^{[A]} \right| = \sqrt{\left(x_i^{[B]} - x_i^{[A]} \right)\left(x_i^{[B]} - x_i^{[A]} \right)} \tag{2}$$

Contact relative displacement U^n is represented as:

$$U^n = \begin{cases} R^{[A]} + R^{[B]} - d & (\text{particle - particle}) \\ R^{[b]} - d & (\text{particle - boundary}) \end{cases} \tag{3}$$

In the formula, $R^{[A]}$ and $R^{[B]}$ are the radius of particles

A and B, respectively. The contact point of two particles is determined by the following expression:

$$x_i^{[C]} = \begin{cases} x_i^{[A]} + \left(R^{[A]} - \frac{1}{2}U^n \right) n_i & (\text{particle - particle}) \\ x_i^{[b]} + \left(R^{[b]} - \frac{1}{2}U^n \right) n_i & (\text{particle - boundary}) \end{cases} \tag{4}$$

Total contact force is decomposed into tangential component and normal component along the contact surface:

$$\overline{F}_i = \overline{F}_i^{\,n} + \overline{F}_i^{\,s} = \overline{F}^{\,n} n_i + \overline{F}^{\,s} t_i \tag{5}$$

In the formula, $\overline{F}_i^{\,n}$ is normal component and $\overline{F}_i^{\,s}$ is tangential component; $\overline{F}^{\,n}$ is normal force scalar and $\overline{F}^{\,s}$ is tangential force scalar. $\overline{F}_i$ and $\overline{M}_3$ are initialized to zero when the connection is formed later, elastic force and torque increment in the contact caused by the displacement increment and rotational increment will be stacked in the current value. Within one time step Δt, the elastic force increment is:

$$\begin{cases} \Delta F_i^{\,n} = \left(-\overline{k}^{\,n} A \Delta U^{\,n} \right) n_i \\ \Delta F_i^{\,s} = -\overline{k}^{\,s} A \Delta U^{\,s} t_i \end{cases}$$

$$\Delta U_i = V_i \Delta t \tag{6}$$

In the formula, $\overline{k}^{\,n}$ is normal connection stiffness and $\overline{k}^{\,s}$ is tangential connection stiffness; $\Delta U^{\,n}$ and $\Delta U^{\,s}$ are normal relative displacement increment and tangential relative displacement increment respectively between two contacting particles within one time step Δt.

$$\begin{aligned} V_i &= \left(\dot{x}_i^{[C]} \right)_{\Phi^2} - \left(\dot{x}_i^{[C]} \right)_{\Phi^1} \\ &= \left(\dot{\boldsymbol{x}}_{\boldsymbol{i}}^{\left[\Phi^2\right]} + \boldsymbol{e}_{\boldsymbol{ijk}} \omega_{\boldsymbol{j}}^{\left|\Phi^2\right|} \left(\boldsymbol{x}_{\boldsymbol{k}}^{[C]} \right) - \boldsymbol{x}_{\boldsymbol{k}}^{\left[\Phi^2\right]} \right) \\ &\quad - \left(\dot{\boldsymbol{x}}_{\boldsymbol{i}}^{\left[\Phi^1\right]} + \boldsymbol{e}_{\boldsymbol{ijk}} \omega_{\boldsymbol{j}}^{\left[\Phi^1\right]} \left(\boldsymbol{x}_{\boldsymbol{k}}^{[C]} - \boldsymbol{x}_{\boldsymbol{k}}^{\left[\Phi^1\right]} \right) \right) \end{aligned} \tag{7}$$

In the formula, $\dot{x}_i^{[\Phi^j]}$ and $\omega_i^{[\Phi^j]}$ are instantaneous speed and instantaneous rotational speed of particles Φ^j respectively. The Φ^j can be determined by the following formula:

$$\left\{ \Phi^1, \Phi^2 \right\} = \begin{cases} \{A, B\} & (\text{particle - particle}) \\ \{B, w\} & (\text{particle - boundary}) \end{cases} \tag{8}$$

Within one time step Δt, the elastic torque increment is:

$$\begin{cases} \Delta \overline{M}_i^{\,n} = \left(-\overline{k}^{\,s} J \Delta \theta^n \right) n_i \\ \Delta \overline{M}_i^{\,s} = -\overline{k}^{\,n} I \Delta \theta_i^s \\ \Delta \theta_i = \left(\omega_3^{[B]} - \omega_3^{[A]} \right) \Delta t \end{cases} \tag{9}$$

In the formula, A is contacting connection area; J is polar moment of inertia of contact surface; I is moment of inertia of contact surface relative to the contact point along the $\Delta\theta_i^s$ -axis direction. Parameters above can be determined by the following formula:

$$\begin{cases} \boldsymbol{A} = \pi \overline{\boldsymbol{R}}^2 \\ \boldsymbol{J} = \frac{1}{2} \pi \overline{\boldsymbol{R}}^4 \\ \boldsymbol{I} = \frac{1}{4} \pi \overline{\boldsymbol{R}}^4 \end{cases} \tag{10}$$

Through the force and torque between particles A and B, calculating the maximum tensile stress and maximum shear stress of connection:

$$\begin{cases} \sigma_{\max} = -\frac{\overline{F}^{\,n}}{A} + \frac{\left| \overline{M}_i^{\,s} \right|}{I} \overline{R} \\ \tau_{\max} = \frac{\left| \overline{F}^{\,s} \right|}{A} + \frac{\left| \overline{M}^{\,n} \right|}{J} \overline{R} \end{cases} \tag{11}$$

In the above equation, when the inequality is equal, namely, the maximum tensile stress $\sigma_{\max}$ is equal to normal strength $\overline{\sigma}_c$. The maximum shear stress $\tau_{\max}$ is equal to shear strength $\overline{\tau}_c$.

Under the rainfall condition at time t, the value of $\overline{\sigma}_c^t$ and $\overline{\tau}_c^t$ are defined as:

$$\psi^t = (1 - \xi^t) \psi^0 \tag{12}$$

In the formula, ψ^0 is the original value of $\overline{\sigma}_c$ and $\overline{\tau}_c$. ξ^t is the relative change rate after rainfall. This data is weakened due to rainfall parameters.

When the maximum tensile stress and maximum shear stress exceed the normal strength and shear strength, namely, $\sigma_{\max} \geq \overline{\sigma}_c$ and $\tau_{\max} \geq \overline{\tau}_c$, bond damage will happen. Normal damage and shear damage variable are defined as:

$$\begin{cases} D^n = \left(U_t^{\,n} - U_{Ts}^{\,n} \right) / \left(U^{\,n} - U_{Ts}^{\,n} \right) \\ D^s = \left(U_t^{\,s} - U_{Ts}^{\,s} \right) / \left(U^{\,n} - U_{Ts}^{\,s} \right) \end{cases} \tag{13}$$

In the formula, U_t^n and U_t^s are normal displacement and shear displacement of the particles respectively at t moment. The damage variable is 0 when the relative displacement reaches threshold displacement, and its value will become 1 when the relative displacement reaches U^n. The normal stiffness $\bar{k}^n$ and tangential stiffness $\bar{k}^s$ at damage stage are calculated by the following formula:

$$\begin{cases} \bar{k}_D^n = (1 - D^n)\bar{k}^n \\ \bar{k}_D^s = (1 - D^s)\bar{k}^s \end{cases} \quad (14)$$

When the maximum tensile stress and maximum shear stress is smaller than normal strength and shear strength, the connecting force and torque among particles will be applied to the connecting particles A and B respectively. The expression is:

$$\begin{cases} \bar{F}_i^{[A]} = \bar{F}_i^{[A]} - \bar{F}_i \\ \bar{F}_i^{[B]} = \bar{F}_i^{[B]} + \bar{F}_i \end{cases} \quad (15)$$

$$\begin{cases} \bar{M}_3^{[A]} = \bar{M}_3^{[A]} - \bar{M}_3 \\ \bar{M}_3^{[B]} = \bar{M}_3^{[B]} - \bar{M}_3 \end{cases} \quad (16)$$

In the formula, $\bar{F}_i^{[A]}$ and $\bar{F}_i^{[B]}$ are the force of particles A and B; $\bar{M}_3^{[A]}$ and $\bar{M}_3^{[B]}$ are the torque of particles A and B.

When shear stress is stronger than yield stress, the particle begins to flow and stress would reduce. Its translational motion and rolling movement mainly depends on the force and bending moment. The velocity and direction of the particle are controlled by the integral calculation from Newton's law. The resultant force and translational motion satisfy the following equation:

$$\bar{F}_i = m(\ddot{x}_i - g_i), \quad (17)$$

where, m is quality, $\ddot{x}_i$ is accelerated velocity, and g_i is acceleration vector of volume force. $\bar{F}_i$ is resultant force on the particle that can be expressed as the following:

$$\bar{F}_i = \bar{F}_i^n + \bar{F}_i^s = \bar{F}^n n_i + \bar{F}^s t_i, \quad (18)$$

where, $\bar{F}_i^n$ is normal component, $\bar{F}_i^s$ is tangential component, $\bar{F}^n$ is scalar normal component of force, and $\bar{F}^s$ is scalar tangential component of force; n_i and t_i are unit normal component and unit tangential component, respectively.

Resultant moment and rotation movement are satisfied in the following relation:

$$\bar{M}_3 = I\dot{\omega}_3, \quad (19)$$

where, I is inertia moment; $\dot{\omega}$ is vector of angular acceleration.

The acceleration of the particle at time *t* can be obtained by central difference method:

$$\begin{cases} \ddot{x}_i^{(t)} = \dfrac{\dot{x}_i^{(t+\Delta t/2)} - \dot{x}_i^{(t-\Delta t/2)}}{\Delta t} \\ \dot{\omega}_3^{(t)} = \dfrac{\dot{\omega}_3^{(t+\Delta t/2)} - \dot{\omega}_3^{(t-\Delta t/2)}}{\Delta t} \end{cases}. \quad (20)$$

Translational velocity and angular velocity at time $(t + \Delta t/2)$ can be achieved by substituting Equation (4) into Equations (1) and (3), respectively:

$$\begin{cases} \dot{x}_i^{(t+\Delta t/2)} = \dot{x}_i^{(t-\Delta t/2)} + (\bar{F}_i^{(t)}/m + g_i)\Delta t \\ \omega_3^{(t+\Delta t/2)} = \omega_3^{(t-\Delta t/2)} + (\bar{M}_3^{(t)}/I)\Delta t \end{cases}. \quad (21)$$

The center position of the particle at time $(t + \Delta t/2)$ can be obtained by Equation (21):

$$x_i^{(t+\Delta t)} = x_i^{(t)} + \dot{x}_i^{(t+\Delta t/2)}\Delta t. \quad (22)$$

The parameters such as translational velocity ($\dot{x}_i^{(t+\Delta t)}$) and rotational velocity ($w_i^{(t+\Delta t)}$), particle's position ($x_i^{(t+\Delta t)}$), force ($F_i^{(t+\Delta t)}$) and moment ($M_3^{(t+\Delta t)}$) on particles at next moment can be achieved by loop iteration process of the method.

Based on constitutive model of particles, the author wrote a ***c++*** program to establish user-defined constitutive model. Dynamic link library (DLL) file was output and called in the main particle discrete element program.

DYNAMIC SIMULATIONS

2D simulations

In order to study the geological disasters of the rock collapse and debris flow induced by rainfall, a 2D rock

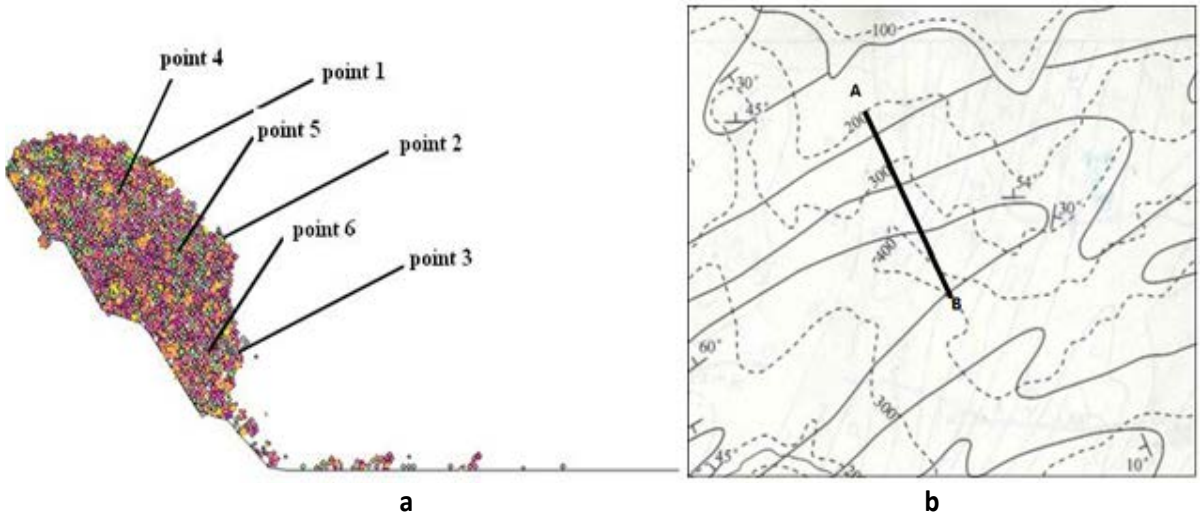

Figure 1. The model of rock collapse (a) Two dimensional model (b) Plan of the area (1:25000).

Table 1. Geotechnical parameters.

Variables \ Model	Initial value of 2D Model	Initial value of 3D Model	Relative change rate of parameters after rain
Normal stiffness / (N/m)	3e7	4.5e7	-14.07
Tangential stiffness / (N/m)	3e7	4.3e7	-14.07
Normal intensity /(N)	2.5e7	3.1e7	-21.13
Tangential intensity /(N)	2.5e7	3.2e7	-21.13
Density/(kg/m^3)	2600	2600	+10.00
Coefficient of friction	0.6	0.6	-11.00

model was established. Laoshan area in Nanjing has a high incidence of debris flow under rainfall that will clog roads and other construction facilities. Figure 1b shows the plan of the partial area of Laoshan area in Nanjing. The authors have done experiments detection. The test results contrasting 2D numerical results were shown in Figure 5.

The 2D numerical model is 110 m long and 30 m high. According to the initial void ratio with 0.1, particle generates randomly in the slope area and its radius changes within 4~6 cm. The contact mechanics parameters of microscopic particles have greater influence on the macroscopic mechanical properties. The mechanics parameters shown in Table 1 have been analyzed by author (Zhao et al., 2013), wherein the relative change rate of each index after rain refers to literature (Li et al., 2009). In the initial state, the 2D model was stable. After fully rainfall, the parameters of rock were weakened. The initial damage data of stiffness was 0.1407. This value was substituted into Equation (14), the rainfall stiffness value were calculated. The change rate of intensity was 0.2113. Then the data of ξ^t was substituted into Equation (12), the rainfall intensity could be calculated. The overall strength of rock mass was induced by initial damage weakening, which resulted in the late rock collapse and debris flow.

The weakening of parameters in the damage process of rock mass follows the constitutive equation. Rock collapse model was shown in Figure 1a. Six different monitoring points on the slope surface and internal points were set to monitor and track motion of particles, the stress and deformation, respectively. There were three sections to monitor the total discharge of debris flow. Frist section is at the toe. Every five meters were set two sections in its base.

The top of the model slope is seen as the origin of coordinates, the vertical downward is negative and the horizontal position to the right is positive. Due to rainfall infiltration, index of shear strength of rock mass significantly became lower. The instability of rock mass would be damaged under the action of gravity, and change of vertical position was negative.

Figure 2 presents curves of vertical location versus time with monitoring points. There are many differences

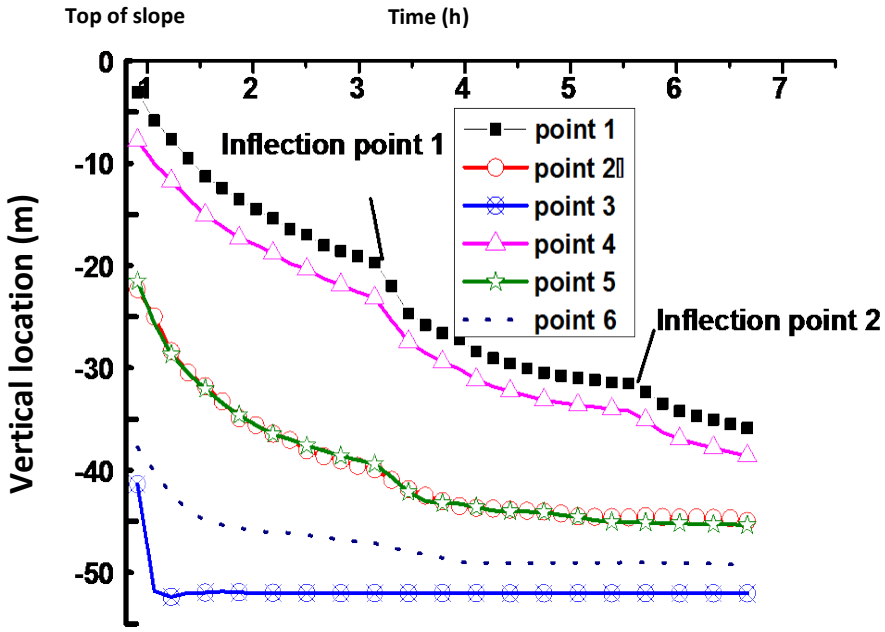

Figure 2. Curves of vertical location versus time with different monitoring points.

among them with rock collapse-damage fracture-debris flow. The processes of rock collapse and debris flow were shown in Figure 3. Taking the movement of Point 1 as an example, before turning inflection Point 1, the bonding force between the particle and adjacent particles were strong. With the process of collapse, the particle collided with other particles and the bedrock, and then damage and fractures where generated at inflection Point 1. Then the evolutionary phase came. The results showed that not all particles of rock mass were damaged and fractured; those unbroken particles mainly depended on their weight and moved along with others. Often this part of rock mass is large, and would have great impact on the downstream.

Figure 3(a)-(e) present three stages of slope failure and evolution: (1) slope with overall stability; (2) initiation and perforation of sliding surface of slope; (3) evolution of debris flow. When time is before 0.8 h and the calculation step is 2.7×10^4, slope is at the stable stage. Loose blocks which attached on the slope, dropped to the slope toe under the action of weight, while some particles dropped a little farther away from the slope toe (Figure 3 (a)). When time reached 1.5 h, the slope was at the early stage of sliding and connection between particles turned from damaging to fracturing gradually. Micro sliding surface first appeared at Point 3, with large angular velocity and speed horizontally along the slope surface which weakened integral strength of the slope. When time reached 3.5 h, debris flow moved with a good liquidity.

Due to the particles at monitoring Point 3 was located outside of the rock cliffs and the lower was impending, they fell early under the influence of weight (Figure 4). When time is 1.5 h, the monitoring point presents the large angular velocity and horizontal velocity. The characteristics of nonlinear motion of slope slide and debris flow is obvious. The main reason is that at early collapse of rock mass, the particles which were connected by the coherence force first collapsed and then collided with adjacent rock in the whereabouts particles, and then the path changed. According to different rotation directions of particles in the process of movement, the clockwise rotation is positive, counterclockwise rotation is negative. In the early stage of debris flow, nonlinear motion was also obvious. However, the motion tended to be stable in later evolution of debris flow. This is because the broken grain went into the hole among large particles, the overall porosity reduced, and then the overall viscosity increased.

The comparison was shown in Figure 5 between the simulation and the experiment. From Figure 5(a), the three section total discharge simulation results agree with the experimental results. Before 2 h, the three section numerical simulation results agreed with experimental results. Then total discharge and impact pressure results were slightly larger than the experimental values in Section 1. Debris flow total discharge results slightly smaller than the experimental values in Section 2. Although, there were some fluctuations, but the overall were regularity. Figure 5(b) presents that in Section 1, 1.9 h occurred at the peak impact pressure 2915KN, then the intensity values produce small fluctuations. It was suggested that the time rate of change of flow rate reaches a maximum debris flow. In the other two

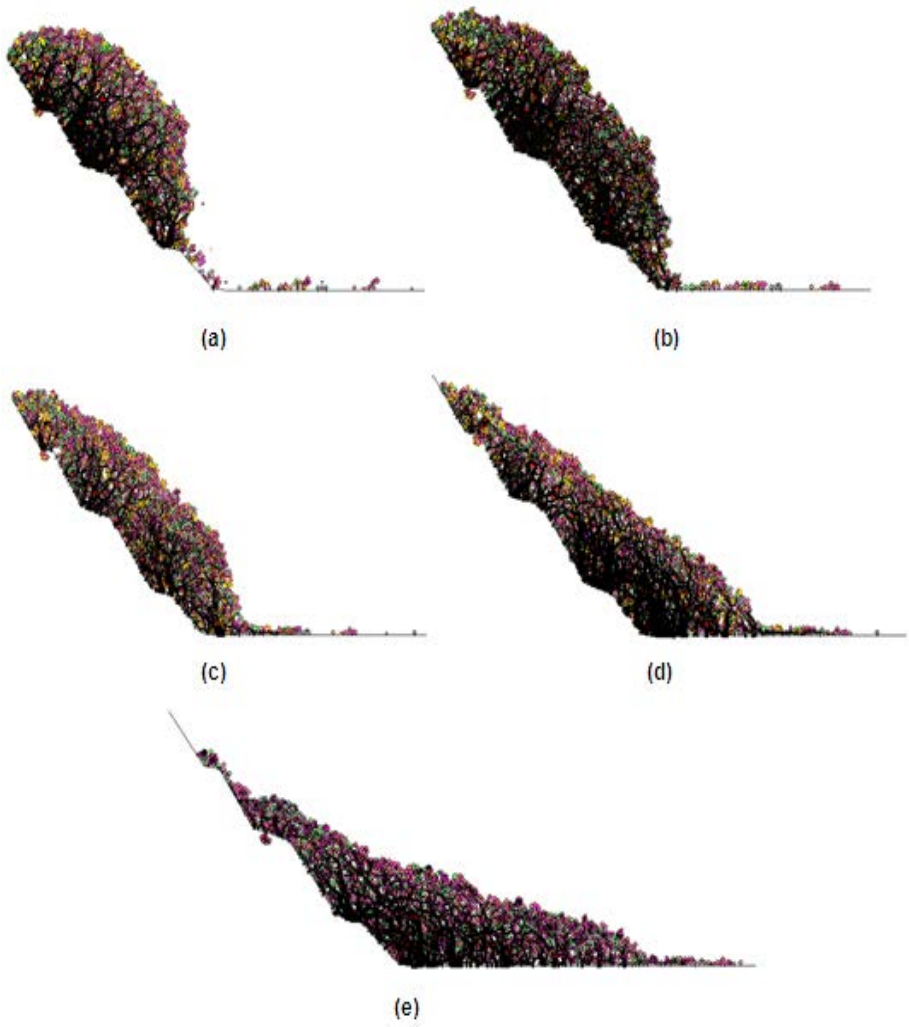

Figure 3. 2D simulation of rock collapse and debris flow. (a) Early rock collapse (b) Stage of rock collapse (c) Early evolution of debris flow (d) Middle evolution of debris flow (e) Stable accumulation of debris flow.

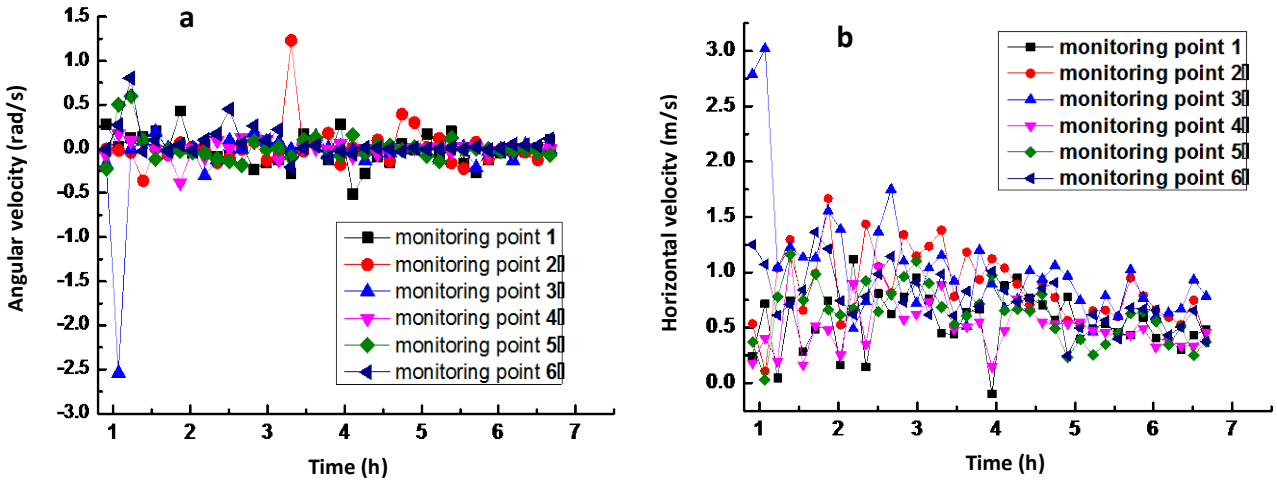

Figure 4. Curves of velocities of monitoring points versus time (a) Angular velocity (b) Horizontal velocity.

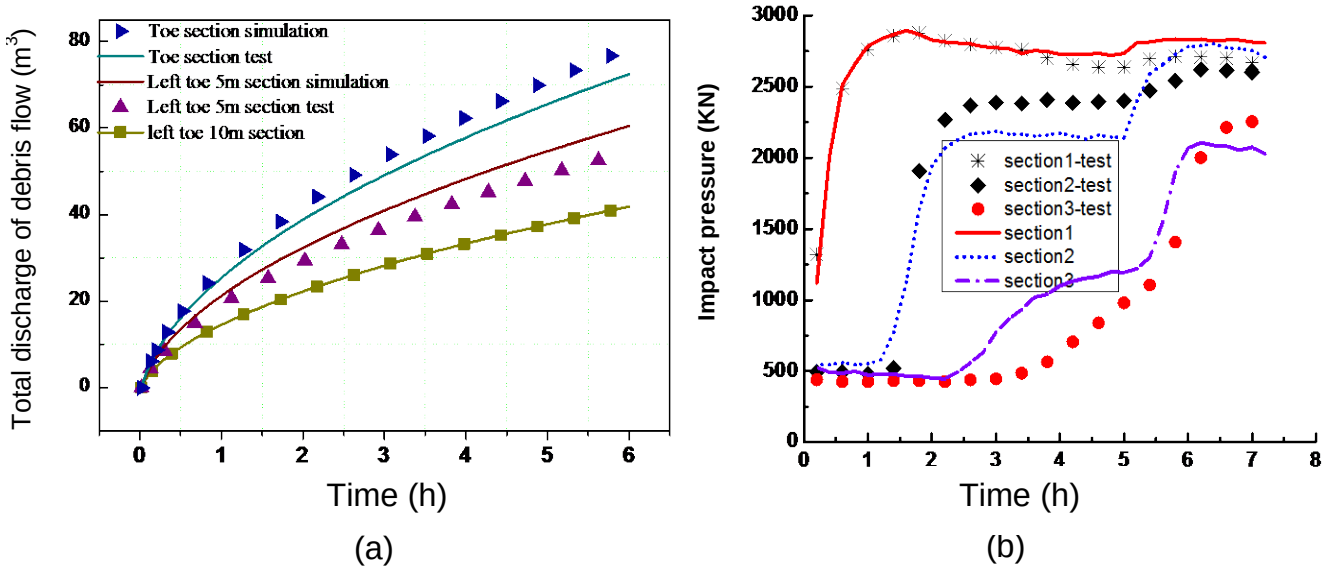

Figure 5. The comparison between the simulate and real landslide test (a) total discharge (b) impact pressure.

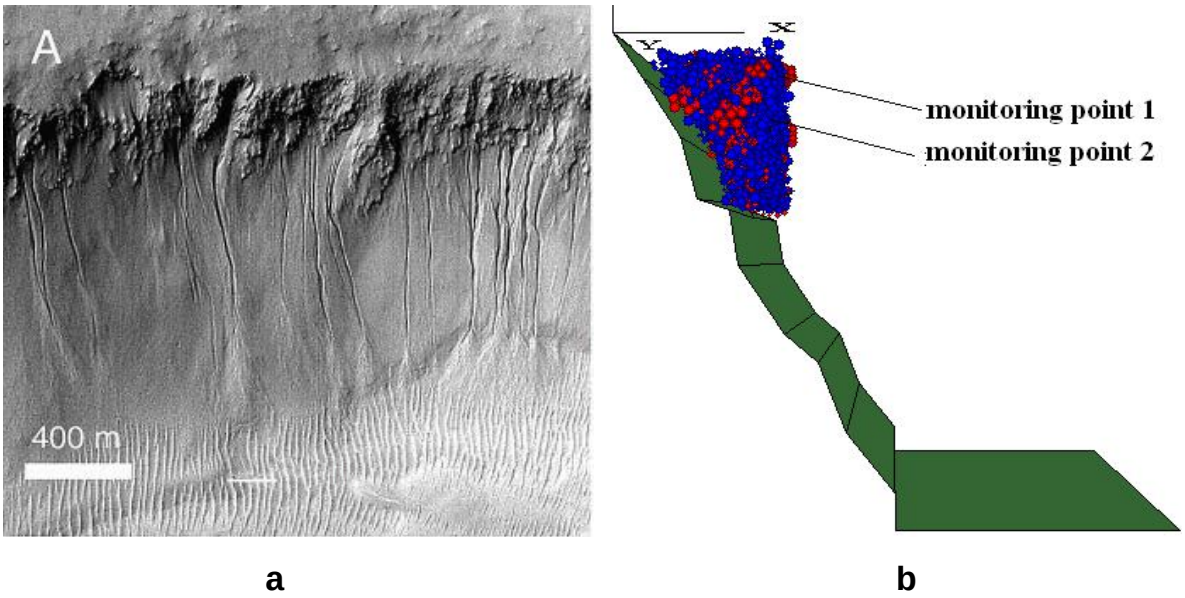

Figure 6. 3D DEM of rock collapse (a) Rock mass collapse of Greenland (b) Rock mass collapse of 3D rock model.

sections, the peak impact pressure was clearly lagging behind, but overall were slight fluctuations up and down in the experimental.

3D simulation studies

In order to study the geological disasters of the rock mass collapse and debris flow induced by rainfall, and compared with debris flow of Greenland in Denmark (Costard et al., 2002), four kinds of 3D models were established. They are 60 m wide and 150 m high. The slopes of bedrock are 1.0, 1.5, 2.0 and 2.5, respectively (Figure 6). According to the initial void ratio with 0.1, particle generated randomly in the slope area and its radius changes within 2~8 cm. The mechanics parameters were also shown in Table 1. In the initial state, the 3D model was stable. The particles within the boundary two XY displacements is constrained in the Z direction, and is allowed to occur displacement

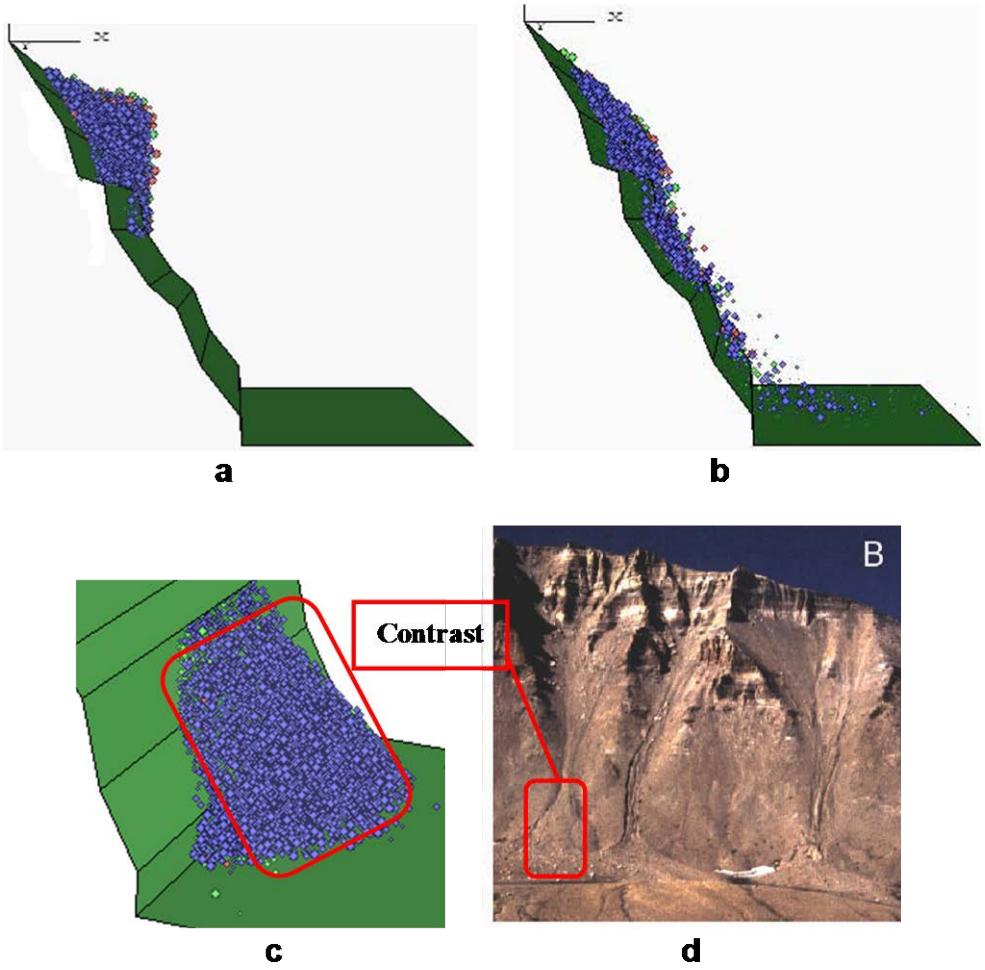

Figure 7. 3D simulation of rock collapse and debris flows (a) Stage of slope slide (b) Stage of debris flow (c) Accumulation of numerical simulation (d) Accumulation of Greenland.

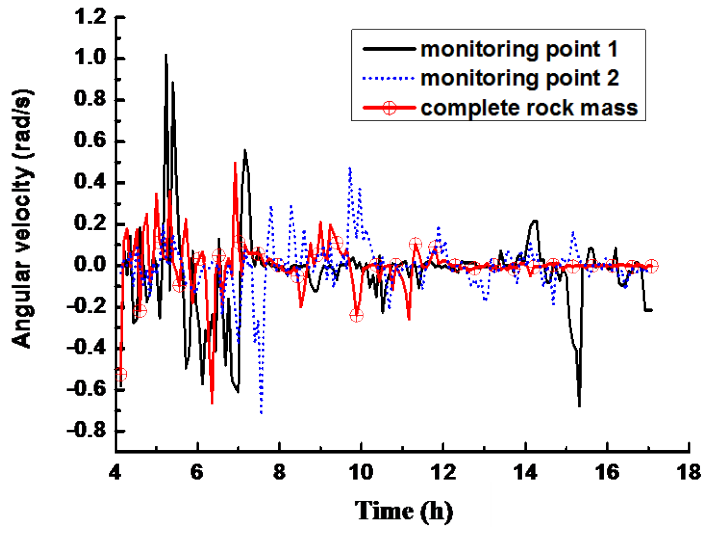

Figure 8. Curves of angular velocity of monitoring points versus time.

movement in the XY plane. After fully rainfall, the parameters of rock were weakened. The initial damage data of stiffness was 0.1407. A weakening of the parameters at this time was 0.2113. The overall strength of rock mass was induced by initial damage weakening, which resulted in the late rock collapse and debris flow.

Two monitoring points in the slope were set to monitor and track displacement and velocity. The processes of rock mass collapse and debris flow were shown in Figure 7. There are also three stages: (1) slope with overall sliding; (2) stage of breaking and rolling; (3) evolution of debris flow. By comparison, the deposition form of numerical simulation agrees with Greenland's form. Figure 7 presents that integrity of the slope is strong at the beginning of the slope slide and the whole rolling of the slope body occurred on the surface of the bedrock.

Figure 8 shows the curves of angular velocity of monitoring points versus time. The angular velocity in clockwise is positive and in counterclockwise is negative. In early slide, the angular velocity is about 0.2 rad/s.

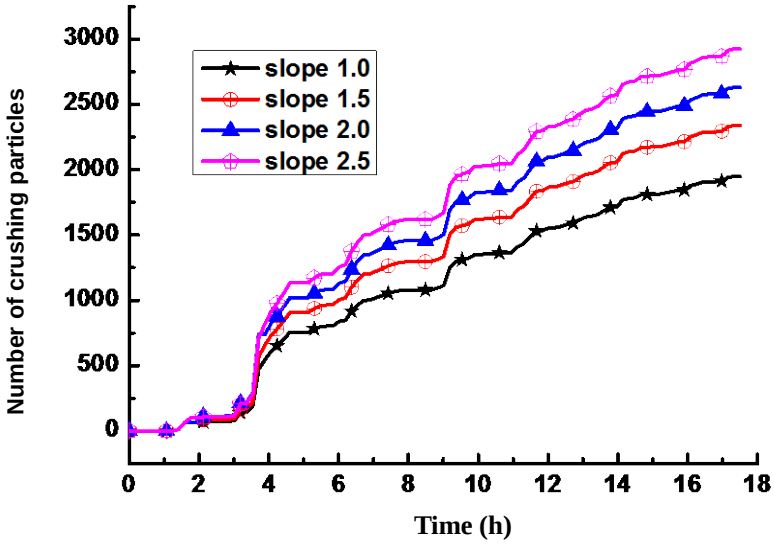

Figure 9. Curves of number of crushing particles versus time under different slope.

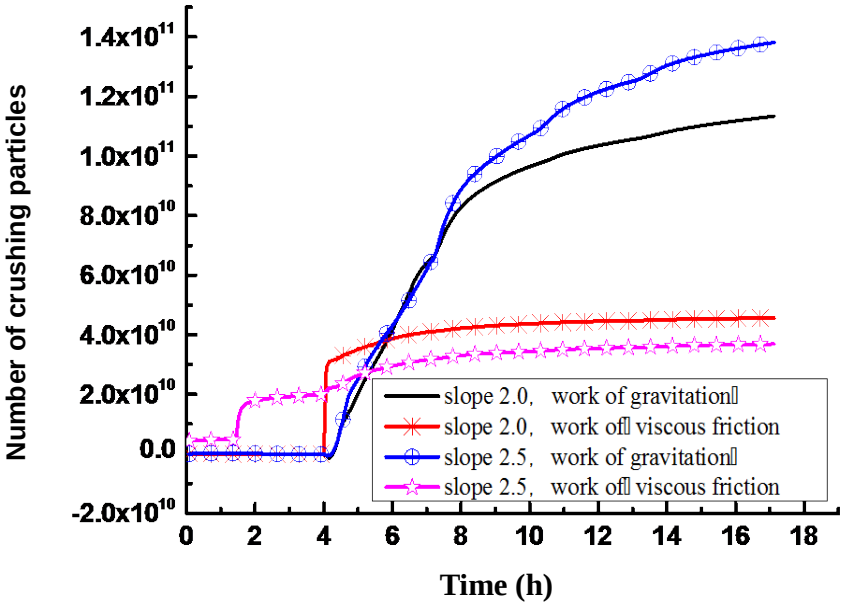

Figure 10. Curves of work of gravitation and viscous friction versus time, respectively.

However, individual rock rolled obviously, such as at 5.2 h, peak value of roll angular velocity of point 1was approximately 1.0 rad/s.

Figure 9 presents that within less than 4 h, number of crushing particle has nothing to do with slope because the aggregate particles are damaged by particle collision force in the prophase of evolution. However, as time went on, energy for decline was released, so the number of crushing particles and slope increased the linear after 4.2 h.

The rock rolled along colliding downstream, the slope body itself would be broken and generated about 81 particles, which is shown on the curve at 4 h in Figure 9. The whole strength of the slope body decreased as well as the cohesive strength. The curve of work of gravitational force in 4~8 h (Figure 10) shows that partial block separated and increment of gravity power was obvious. Later in the process of debris flow, it continued to flow along the bedrock, glutinousness and viscosity increased; the angular velocity of rock mass is close to

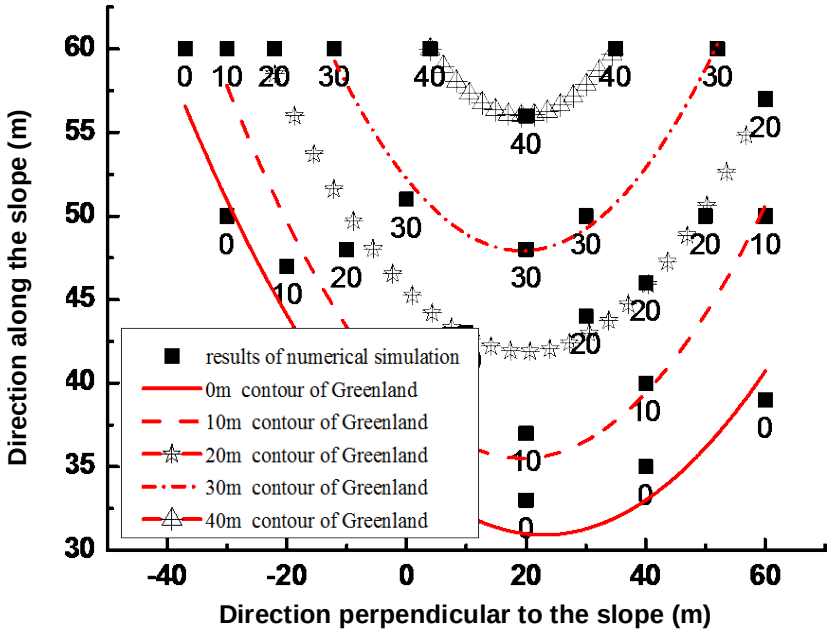

Figure 11. Contours of accumulation body of numerical simulation and of Greenland.

zero (Figure 8). The curves of work of friction that produced by the viscous force are flat (Figure 10) in this phase. Then, debris flow reached the bottom of the bedrock with the advancement of upstream particles layered erosion accumulation was generated by front-end particles (Figure 11).

Figure 11 presents the contrast between contours of accumulation body by the numerical simulation and Greenland when the slope is 2.5. The numerical 0 and 10 m contours in front of accumulation area were slightly smaller than that of Greenland. The main reason is that in simulation, the established rock particles are sphere particles, the porosity of accumulated particles are large; while the density of actual rock mass is great after medium-sized particles filled the voids among large particles in the process of debris flow resulting in flat deposits. Taken together the contours of accumulation body by simulation fit in geological disasters of Greenland, so the rationality of the model has been verified.

Figure 12 presents the increase of slope, displacement and the speed of monitoring points along the slope present nonlinear trend for increasing. When the slope increases from 1.0 to 2.0, the curves of displacement increase by linear ratio. When the slope increases from 2.0 to 2.5, displacement and velocity increase significantly. Under the same slope, nonlinear motion of displacement and the speed of monitoring points are obvious. The reason is that the collision among particles and crushing changed their trajectory and orientation which would affect the displacement and velocity components. The above explain that the nonlinear characteristic of microscopic particles is closely combined with macroscopic changing process of rock mass.

DISCUSSION

After a rainfall, there is rock collapse and the occurrence and debris flow evolution of geological disasters. Research on this problem has great superiority by discrete element method. This method can be used to study micro body particle movement. Real time tracking effect is good. However, there are still problems and needs improvement.

In the debris flow motion process, further research needs associated with slurry. In Figure 5, the two-dimensional simulation results and experimental results of node factors exist differences in slurry.

Numerical simulation of the discrete element method can achieve large-size 3D slope model at the same time need to generate a lot of particles. However, the calculation takes more computing time is currently drawbacks. How to achieve ultra-performance parallel computing is one of the ways to expand its field of application.

Conclusions

Based on the discrete element method, the article derived the constitutive model of particles connect-damage fracture-move and simulated rock mass collapse and dynamic process of debris flow. The article analyzed

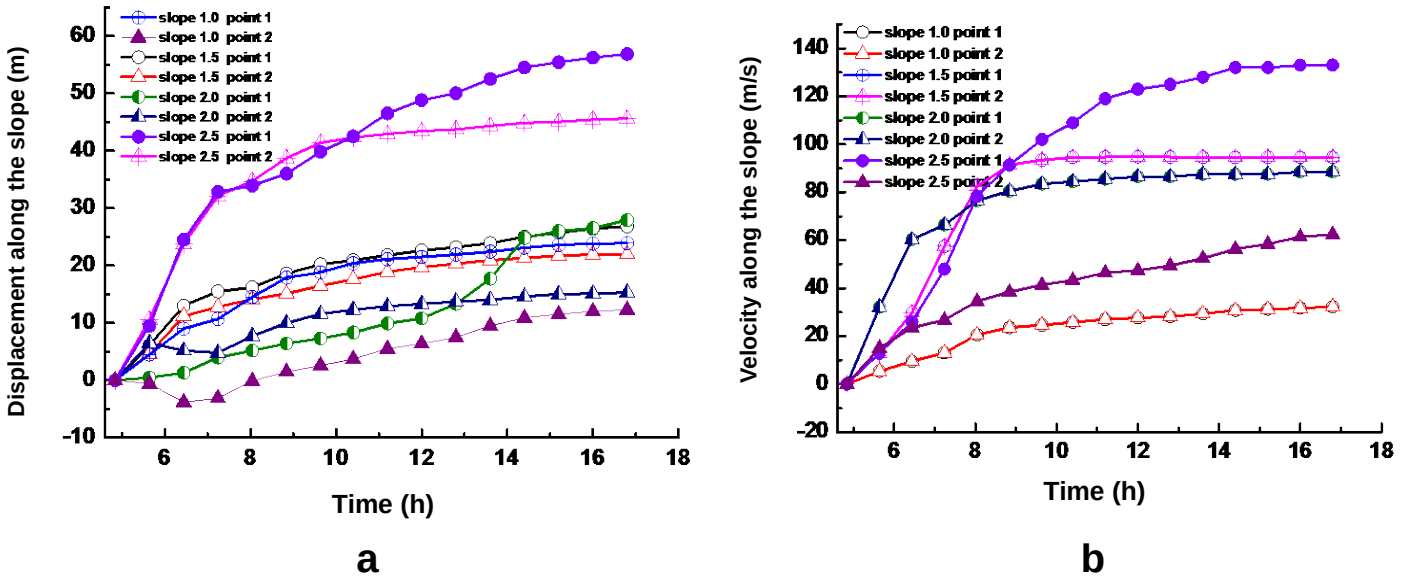

Figure 12. Curves of dynamic parameter of monitoring points versus time (a) Displacement of monitoring points (b) Velocity of monitoring points.

influence of slope of bed rock on parameters of rock mass collapse and debris flow. The article also analyzed the characteristic of nonlinear motion of different monitoring points. The main results are as follows:

(1) The process of rock mass collapse and debris flow is complex kinetic processes, and presents progressive dynamic evolution process from continuum to discontinuous. The experiments of the model have practical significance on engineering to describe the nonlinear motion kinetic characteristics of the whole process of slope,
(2) There are three stages of rock mass collapse and debris flow with different kinetic characteristics. In the evolution of debris flow, slope on cliffs is easy to slide, with great energy and obvious nonlinear movement,
(3) Rainfall is one of the main factors that induce geological disasters. The numerical results agree well with the experimental results. Tracking the evolution of the dynamic parameters of rock particles can compensate experiment deficiencies.

Conflict of Interest

The authors have not declared any conflict of interest.

ACKNOWLEDGMENTS

The authors gratefully acknowledge the financial support by the Natural Science Foundation of Jiangsu Province under grant no. BK2010457 and the National Natural Science Foundation of China under grant no. 51275250.

REFERENCES

Costard F, Forget F, Mangold N, Peulvast JP (2002). Formation of recent Martian Debris Flows by melting of near-surface ground ice at high obliquity. Sci. 295(4):110-113. http://dx.doi.org/10.1126/science.1066698
Fan YY, Wang SJ, Wang EZ, Liu XL (2010). Simulationanalysisofdynamicprocessof entrainmentof path material by debris flow. Chinese J. Rock Mech. Eng. 29(S2):4146-4152.
Federicoa T, Michaele P (2007). Discrete element method for modeling solid and particulate materials. Int. J. Numer. Methods Eng. 70(4):379-404. http://dx.doi.org/10.1002/nme.1881
Iverson R (1997).The physics of debris flows. Rev. Geophysics 35(3):245-296. http://dx.doi.org/10.1029/97RG00426
Jiang JC, Yokino K, Yamagami T (2008). Identification of dem parameters for rockfall simulation analysis. Chinese J. Rock Mech. Eng. 27(12):2418-2430.
Kane I, Ponten A (2012). Submarine transitional flow deposits in the Paleogene Gulf of Mexico. Geol. 40(12):1119-1122. http://dx.doi.org/10.1130/G33410.1
Lei YJ, Wang SHL (2006). Stability analysis of jointed rock slope by strength reduction method based on UDEC. Rock Soil Mech. 27(10):1693-1698.
Li KG, Hou KP, Zhang CHL (2009). Experiment study on shear characteristics of saturated rock mass. J. Central South Univ. Sci. Technol. 40(2):538-542.
Li SH H, Liu TP, Liu XY (2009). Analysis method for landslide stability. Chinese J. Rock Mech. Eng. 28(S2):3309-3324.
Mohsin JB, Muhammad U, Raheel Q (2013). Landslide dam and subsequent dam-break flood estimation using HEC-RAS model in Northern Pakistan. Nat. Hazards. 65(1):241-254. http://dx.doi.org/10.1007/s11069-012-0361-8
Neal RI, Denis C, Thomas SH (2003). Effects of Basal Debris on Glacier Flow Sci. 301(4):81-84.
Nicholas TL, Andrew JM, Gordon EG, Paul K (2014). Debris flow initiation in proglacial gullies on Mount Rainier, Washington.

Geomorphol. 226(1):249-260.
Sitharam TG, Vinod JS (2010). Evaluation of shear modulus and damping ratio of granular materials using discrete element approach. Geotechn. Geol Eng. 28(5):591-601.
Tang ZHP, Xu JL (2007). A combined discrete cylindrical shell finite element multiscale method and its application. Chinese J. Comput. Mech. 24(5):591-596.
Wang YN, Fulvio T (2011). Discrete element modeling of rock fragmentation upon impact in rock fall analysis. Rock Mech. Rock Eng. 44(1):23-25. http://dx.doi.org/10.1007/s00603-010-0110-9
Zhang WS, Zhao YX, Cui P, Peng H, Chen XJ (2012).Two-dimensional numerical model for debrisflow motion and gully bed evolution. Sci. Soil Water Conserv. 10(1):1-5.
Zhao JK, Li, H, Zhang HQ (2013). Characteristics study on meso-mechanical models of geotechnical based on discrete element method. J. Disaster Prevent ion Mitigation Eng. 33(2):218-224.
Zhou J, Deng YB, Jia MC, Wang JQ (2010). Coupling method of two-dimensional discontinum based on contact between particle and element. Chinese J. Geotech. Eng. 32(10):1479-1484.

academicJournals

Related Journals Published by Academic Journals

- International NGO Journal
- International Journal of Peace and Development Studies